

Supporting Information: Exploring the disruption of SARS-CoV-2 RBD binding to hACE2

Camryn Carter,^A Justin Airas,^A Haley Gladden,^A Bill R. Miller III,^B and Carol A. Parish^{A,*}

A. Department of Chemistry, Gottwald Center for the Sciences, University of Richmond, Richmond, VA, 23173, USA

B. Department of Chemistry, Truman State University, Kirksville, MO 63501, USA

* Corresponding author

Apo

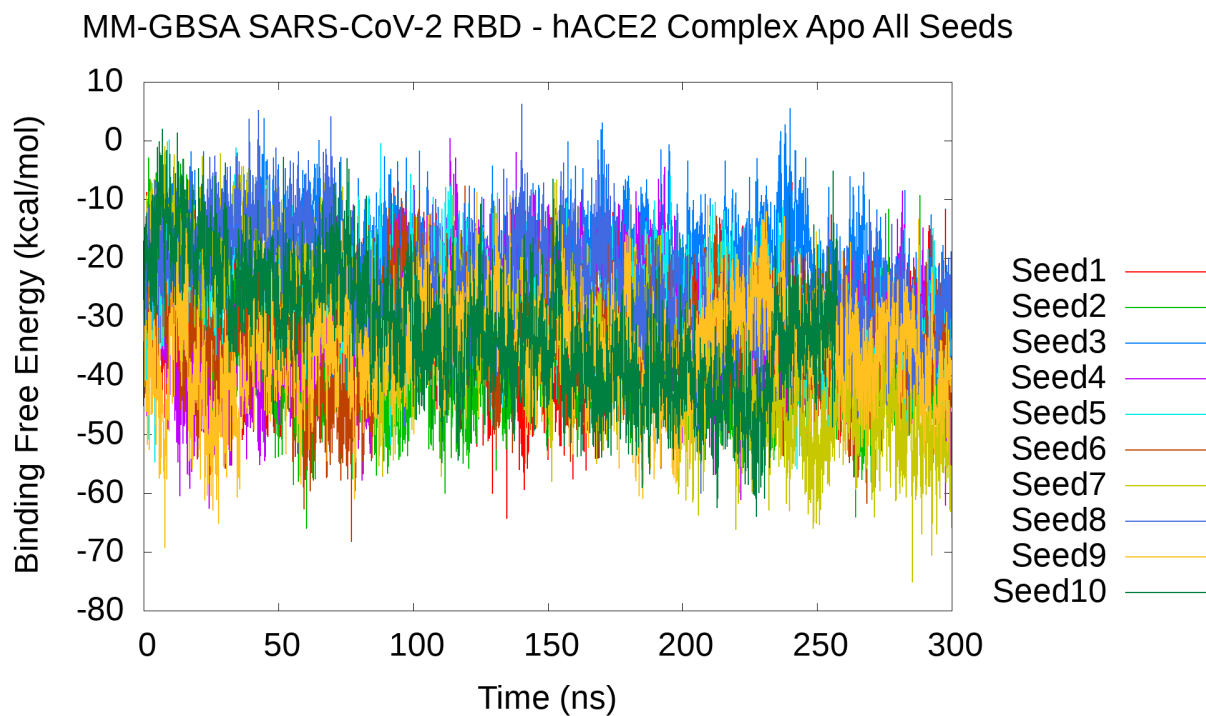


Figure S1. Apo MM-GBSA binding energies for RBD - hACE2 complex. The MM-GBSA binding energies are reported for the entire 300ns simulation and for each seed. The corresponding color for each seed is indicated in the key.

Table S1. Apo MM-GBSA binding energies for each seed. The average MM-GBSA binding energies for all ten seeds across 300ns simulations.

Seeds	Apo MM-GBSA (kcal/mol)	Std Dev. (kcal/mol)	Std. Error (kcal/mol)
-------	------------------------	---------------------	-----------------------

1	-33.69	8.38	0.15
2	-36.83	9.30	0.17
3	-21.11	7.81	0.14
4	-31.84	9.54	0.17
5	-27.93	8.07	0.15
6	-34.36	8.73	0.16
7	-33.56	12.83	0.23
8	-24.74	8.97	0.16
9	-35.60	8.66	0.16
10	-32.60	11.03	0.22

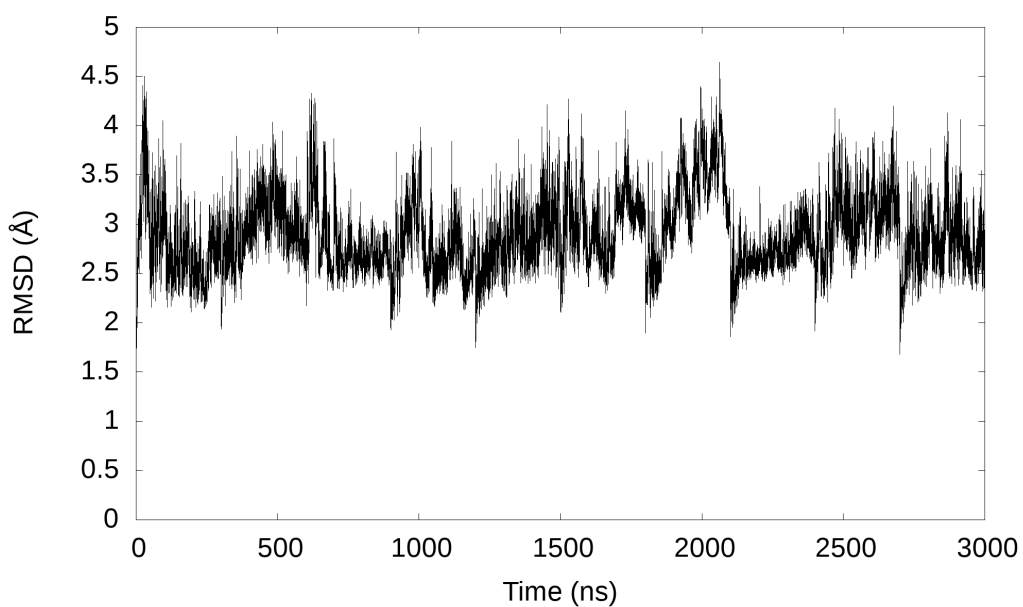


Figure S2. RMSD of SARS-CoV-2 RBD - hACE2 complex. The RMSD is calculated for all residue backbones and side chains for the 3 μ s ensemble.

Table S2. SARS-CoV-2 RBD - hACE2 Apo pairwise decomposition energies. Listed in the table are RBD residues and hACE2 residues, and the corresponding average pairwise decomposition energy. Interactions were selected if pairwise decomposition was less than -2 kcal/mol.

RBD Residue	hACE2 Residue	van der Waals	Electrostatic	Pairwise Decomposition

				Avg. ± Std. Dev. (kcal/mol)
Lys417	Asp30	0.17 ± 0.68	-43.56 ± 7.74	-6.52 ± 2.94
Tyr505	Lys353	-2.21 ± 0.36	-1.63 ± 0.79	-5.00 ± 0.54
Asn501	Lys353	-1.61 ± 0.29	-3.63 ± 2.02	-4.73 ± 1.46
Thr500	Asp355	-0.66 ± 0.59	-3.11 ± 3.25	-4.70 ± 2.44
Gln493	Glu35	-0.47 ± 0.55	-4.74 ± 2.82	-4.49 ± 1.80
Gln493	Lys31	-0.14 ± 0.54	-6.90 ± 3.91	-4.13 ± 1.95
Gln498	Lys353	-0.15 ± 0.46	-4.90 ± 4.84	-3.86 ± 3.30
Tyr449	Asp38	0.09 ± 0.72	-6.08 ± 4.07	-3.59 ± 2.01
Gly496	Lys353	0.10 ± 0.56	-5.17 ± 2.41	-3.25 ± 1.77
Asn487	Tyr83	-0.05 ± 0.55	-3.37 ± 1.39	-2.89 ± 0.96
Asn487	Gln24	-0.96 ± 0.40	-1.25 ± 1.27	-2.87 ± 0.93
Tyr505	Glu37	-0.19 ± 0.61	-4.36 ± 4.32	-2.86 ± 2.38
Phe486	Met82	-1.22 ± 0.42	-0.01 ± 0.27	-2.47 ± 0.78
Asn501	Tyr41	-0.73 ± 0.36	-0.60 ± 0.64	-2.33 ± 1.25
Gln493	His34	-1.02 ± 0.37	-0.83 ± 1.42	-2.12 ± 1.23
Tyr453	His34	-0.54 ± 0.40	-1.60 ± 1.32	-2.07 ± 1.05

Table S3. The average hydrogen bonding occurrences for the 3000 ns ensemble. Below are hydrogen bonding percentages that were greater than 5%.

Acceptor	Donor	Hydrogen Bonding Percent Occurrence (avg.)
RBD - Asn487 @ OD1	hACE2 - Tyr83 @ HH-OH	69.56
hACE2 - Lys353 @ O	RBD - Gly502 @ H-N	66.80
hACE2 - Asp355 @ OD1, OD2	RBD - Thr500 @ HG1-OG1	42.19

hACE2 - Asp38 @ OD1, OD2	RBD - Tyr449 @ HH-OH	59.72
hACE2 - Tyr41 @ OH	RBD - Thr500 @ HG1-OG1	29.37
hACE2 - Glu35 @ OE1, OE2	RBD - Gln493 @ HE21-NE2, HE22-NE2	52.44
hACE2 - His34 @ ND1	RBD - Tyr453 @ HH-OH	24.98
hACE2 - Glu37 @ OE1, OE2	RBD - Tyr505 @ HH-OH	44.40
hACE2 - Gln24 @ OE1	RBD - Asn487 @ HD21-ND2, HD22-ND2	19.62
RBD - Ala475 @ O	hACE2 - Ser19 @HG-OG	17.37
RBD - Gln493 @ OE1	hACE2 - Lys31 @ HZ1, HZ2, HZ3-NZ	36.74
RBD - Gln498 @ OE1	hACE2 - Lys353 @ HZ1, HZ2, HZ3-NZ	34.90
RBD - Ala475 @ O	hACE2 - Gln24 @ HE21-NE2, HE22-NE2	11.76
hACE2 - Asp38 @ OD1, OD2	RBD - Gln498 @ HE21-NE2, HE22-NE2	19.52
hACE2 - Asp30 @ OD1, OD2	RBD - Lys417 @ HZ1, HZ2, HZ3-NZ	57.81
hACE2 - Ala386 @ O	RBD - Tyr505 @ HH-OH	10.08
RBD - Ser494 @ O	hACE2 - His34 @ HE-NE2	9.93
RBD - Gly496 @ O	hACE2 - Lys353 @ HZ1, HZ2, HZ3-NZ	26.47
RBD - Gly446 @ O	hACE2 - Gln42 @ HE21-NE2, HE22-NE2	9.02
RBD - Tyr495 @ O	hACE2 - Lys353 @ HZ1, HZ2, HZ3-NZ	7.75

Table S4. SARS-CoV-2 RBD - hACE2 hydrogen bonds and pairwise decomposition energies.

Hydrogen bonding occurrences for residue interactions between the SARS-CoV-2 RBD and the hACE2 receptor. For each hydrogen bonding interaction represented in the table, the corresponding pairwise decomposition energy of said interaction is listed. Pairwise decomposition is calculated from 30,000 frames from the full 3000 ns ensemble. The table includes hydrogen bonding occurrences greater than 5%.

RBD Residue	hACE2 Residue	Hydrogen Bonding Percent Occurrence (avg.)	Pairwise Decomposition (avg. ± std. dev.) (kcal/mol)
Asn487	Tyr83	69.56	-2.89 ± 0.96
	Gln24	19.62	-2.87 ± 0.93
Gly502	Lys353	66.80	-1.63 ± 0.32
Tyr449	Asp38	59.72	-3.59 ± 2.01
Lys417	Asp30	57.81	-6.52 ± 2.94
Gln493	Glu35	52.44	-4.50 ± 1.80
	Lys31	36.74	-4.13 ± 1.95
Tyr505	Glu37	44.40	-2.86 ± 2.38
	Ala386	10.08	-0.50 ± 0.82
Thr500	Asp355	42.19	-4.70 ± 2.44
	Tyr41	29.68	-1.26 ± 1.46
Gln498	Lys353	34.90	-3.86 ± 3.30
	Asp38	19.52	-1.68 ± 2.27
Gly496	Lys353	26.47	-3.25 ± 1.77
Tyr453	His34	24.98	-2.07 ± 1.05
Ala475	Ser19	17.37	-0.73 ± 1.29

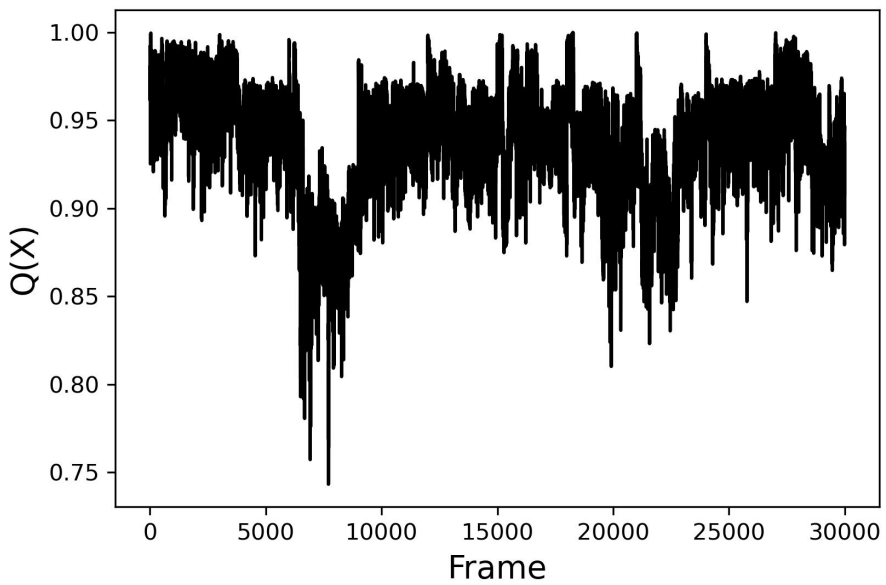


Figure S3. Native contact analysis in the interface of apo 3 μ s ensemble. The fraction of native contacts is plotted for each frame.

Notably, there is a decrease in the fraction of native contacts between frames 6,493 and 8,550, which occurs in seed 3. After visualizing the 3 μ s ensemble, we did not identify a noticeable difference in the SARS-CoV-2 RBD and hACE2 interface during these frames. However, we found a notable decrease in pairwise decomposition energies of residue interactions during seed 3 as compared to the average 3 μ s ensemble, which supports the reduction in the fraction of native contacts. Interactions such as RBD Gln498 - hACE2 Lys353 (-0.18 (0.04) kcal/mol), RBD Gly496 - hACE2 Lys353 (-0.81 (0.07) kcal/mol), RBD Tyr505 - hACE2 Glu37 (-0.37 (0.08) kcal/mol), and RBD Asn501 - hACE2 Tyr41 (-0.37 (0.04) kcal/mol) have low pairwise decomposition energies compared to the average over 10 seeds (Table S2). Notably, seed 3 has the lowest average MM-GBSA binding energy (-21.11 (0.14) kcal/mol), suggesting that this seed sampled a region of the potential energy surface where these interactions were unfavorable (Table S1).

Site Map

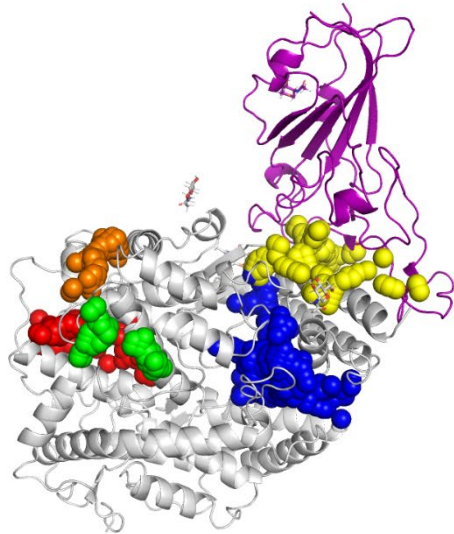


Figure S4. SiteMap results for 6LZG. Blue indicates Site #1 (SScore 1.005, DScore 1.029), yellow indicates Site #2 (SScore 1.002, DScore 1.017), red indicates Site #3 (SScore 1.053, DScore 1.061), green indicates Site #4 (SScore 0.743, DScore 0.742), and orange indicates Site #5 (SScore 0.696, DScore 0.672). Site #2 occurs in the hACE2 – SARS-CoV-2 RBD complex junction and is the binding site of interest.

Table S5. SiteMap properties for 6LZG binding sites.

Site #	Size	Volume	Exposure	Enclosure	Contact	Phobic	Philic	Balance	Don/Acc
1	251	885.28	0.645	0.696	0.352	0.352	1.010	0.348	1.088
2	164	568.35	0.697	0.702	0.854	0.236	1.057	0.223	0.711
3	133	463.74	0.567	0.777	1.008	0.712	1.060	0.672	0.831
4	56	120.05	0.735	0.546	0.685	0.225	0.887	0.254	0.948
5	50	117.65	0.725	0.549	0.737	0.156	0.989	0.158	1.392

Epik and Glide Docking

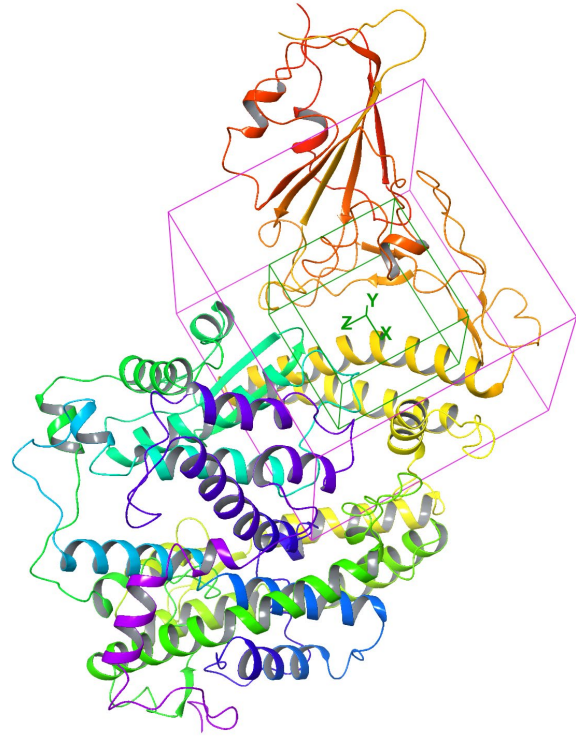


Figure S5. SARS-CoV-2 RBD and hACE2 complex receptor grid for ligand docking.

Table S6. GlideScores of all ligands. A ranking for each ligand is based on the XP GlideScore of the first pose.

Drug Name	6LZG	
	GlideScore (kcal/mol)	Rank
Benazepril	-4.154	8
Captopril	-3.588	13
Enalapril	-4.097	9
Fosinopril	-6.050	2
Fosinoprilat	-3.287	16
Lisinopril	-4.959	3
Lisinopril (-1)	-3.353	15
Perindopril	-3.569	14
Quinapril	-3.984	11
Ramipril	-4.070	10
Trandolapril	-3.643	12
Aloe Emodin LS-H15204	-4.384	7
Camostat LS-H6976	-2.731	17
Emodin LS-H11074	-4.706	5
Emodin LS-H17409	-4.402	6
Physcion LS-H9395	-4.737	4
Diquafosol	-9.138	1

Table S7. Top three poses of each ligand. The top three poses of each ligand and their corresponding GlideScores are listed. The rank was decided based on the GlideScore of the first pose of each ligand.

Rank	Ligands	GlideScore (kcal/mol)
1	Diquafosol P1	-9.138
	Diquafosol P2	-8.914
	Diquafosol P3	-8.406

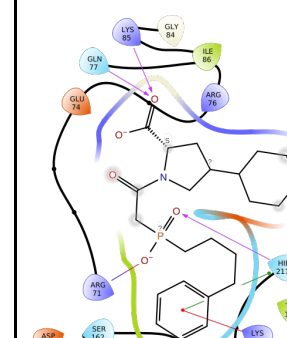
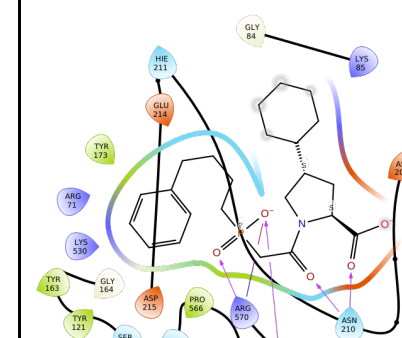
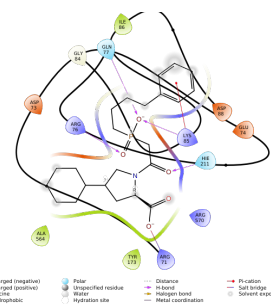
2	Fosinopril P1	-6.050
	Fosinopril P2	-5.683
	Fosinopril P3	-5.675
3	Lisinopril P1	-4.959
4	Physcion P1	-4.737
	Physcion P2	-4.657
	Physcion P3	-4.619
	Lisinopril P2	-4.874
	Lisinopril P3	-4.861
5	Emodin_H11074 P1	-4.706
	Emodin_H11074 P2	-4.542
6	Emodin_H17409 P1	-4.402
7	Aloe Emodin P1	-4.384
	Aloe Emodin P2	-4.316
	Aloe Emodin P3	-4.298
	Emodin_H11074 P3	-4.294
	Emodin_H17409 P2	-4.182
8	Benazepril P1	-4.154
	Benazepril P2	-4.130
9	Enalapril P1	-4.097
10	Ramipril P1	-4.070
11	Quinapril P1	-3.984
	Ramipril P2	-3.928
	Quinapril P2	-3.819
	Enalapril P2	-3.739
	Quinapril P3	-3.730

12	Trandolapril P1	-3.643
	Trandolapril P2	-3.638
	Enalapril P3	-3.631
	Emodin_H17409 P3	-3.618
13	Captopril P1	-3.588
14	Perindopril P1	-3.569
	Benazepril P3	-3.547
	Captopril P2	-3.499
15	Lisinopril NH P1	-3.353
16	Fosinoprilat P1	-3.287
	Trandolapril P3	-3.186
	Perindopril P2	-3.135
	Lisinopril NH P2	-3.087
	Fosinoprilat P2	-3.083
	Captopril P3	-2.925
	Fosinoprilat P3	-2.918
	Lisinopril NH P3	-2.889
	Ramipril P3	-2.882
17	Camostat P1	-2.731
	Benazepril NH P1	-2.666
	Fosinopril P3	-2.608
	Benazepril NH P2	-2.549
	Benazepril NH P3	-2.478
	Camostat P2	-2.316
	Camostat P3	-2.307

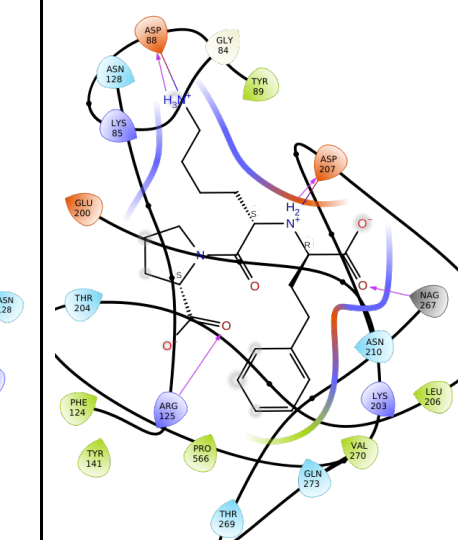
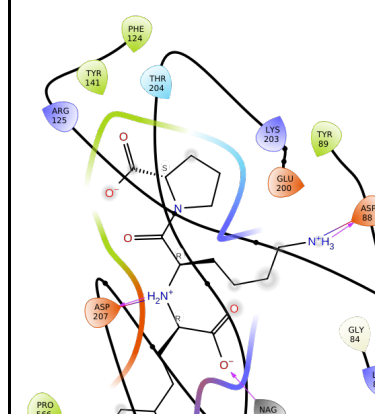
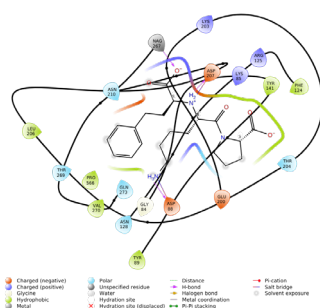
Table S8. Ligand Interaction diagrams. Below includes the ligand interaction diagrams for the top 3 poses of each ligand selected for MD analysis.

Ligands	Pose 1	Pose 2	Pose 3
Diquafosol			
Emodin_H11074			
Fosinopril			

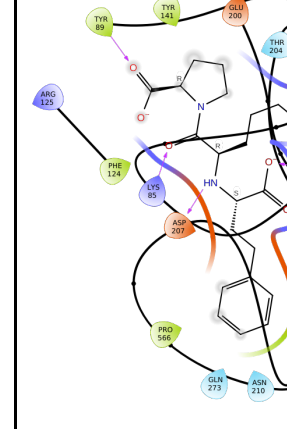
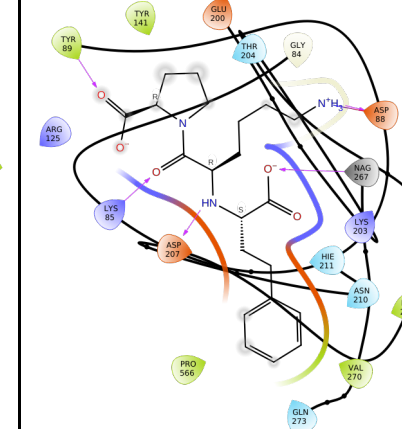
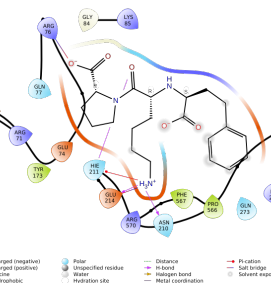
Fosinoprilat

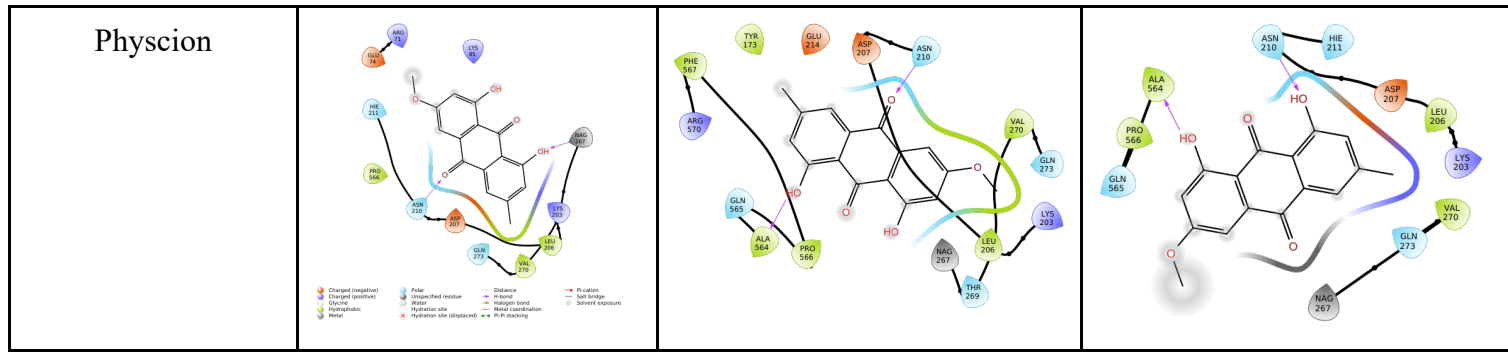


Lisinopril (0)



Lisinopril (-1)





ADME and PAINS

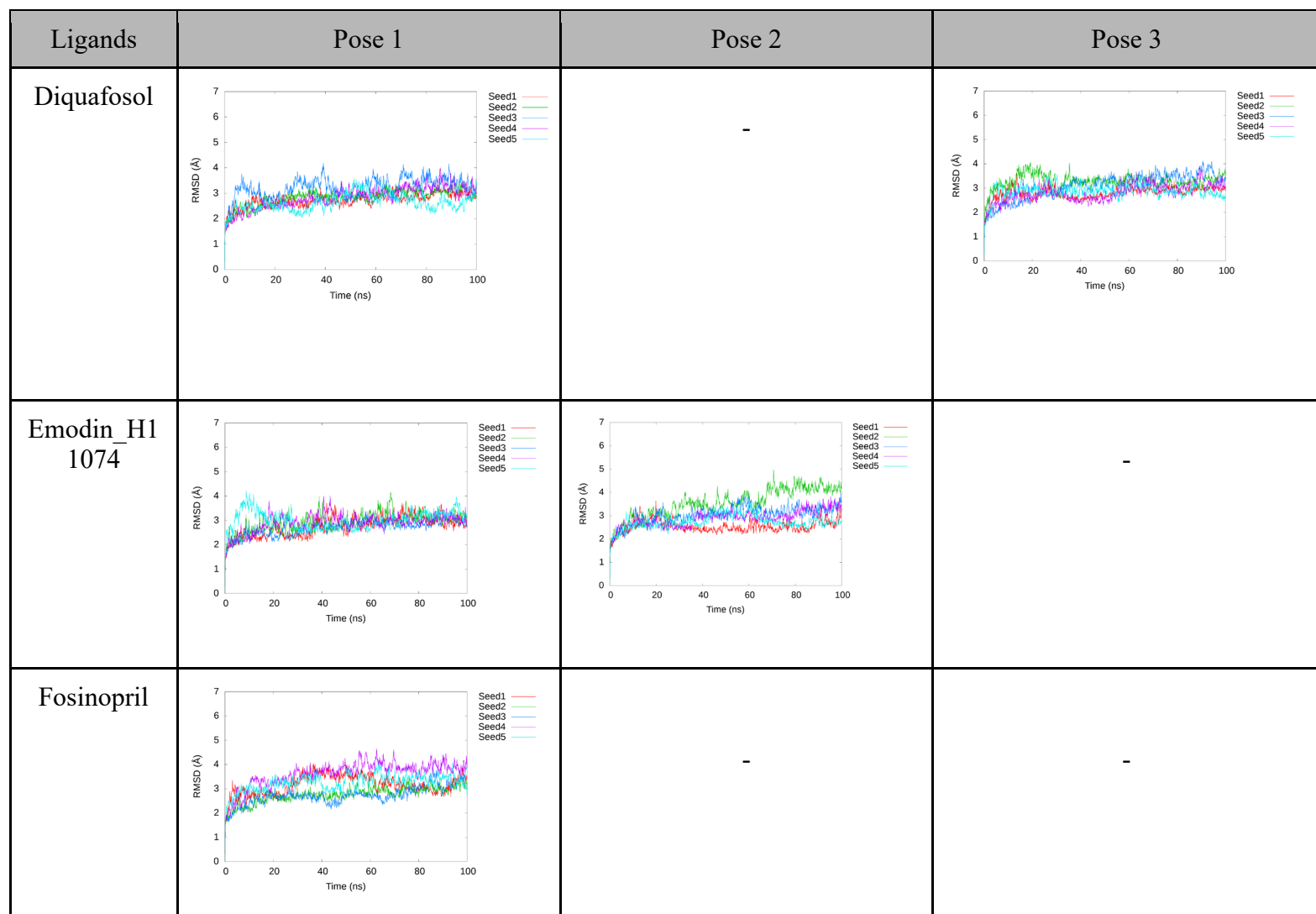
Table S9. ADME properties for seven selected ligands. ADME properties for diquafosol, emodin, fosinopril, fosinoprilat, lisinopril with -NH_2^+ - backbone nitrogen, lisinopril with -NH -backbone nitrogen, and physcion. H-bond donor and acceptor refer to the average number of hydrogen atoms on the molecule that is estimated to be capable of donating or accepting a hydrogen bond, respectively. logP Octanol/Water and logS Aqueous Solubility refers to the solubility of the ligand. logBB Brain/Blood refers to how likely the drug is able to cross the blood-brain barrier. Lastly, logIC₅₀ HERG K⁺ refers to the amount (in log scale) that would need to be taken to block the HERG K⁺ channel. Data that exceeds the range of 95% of known drugs used in the ADME program are underlined, and data that was flagged due to the molecular weight of the ligand exceeding the trained set of compounds is bolded.

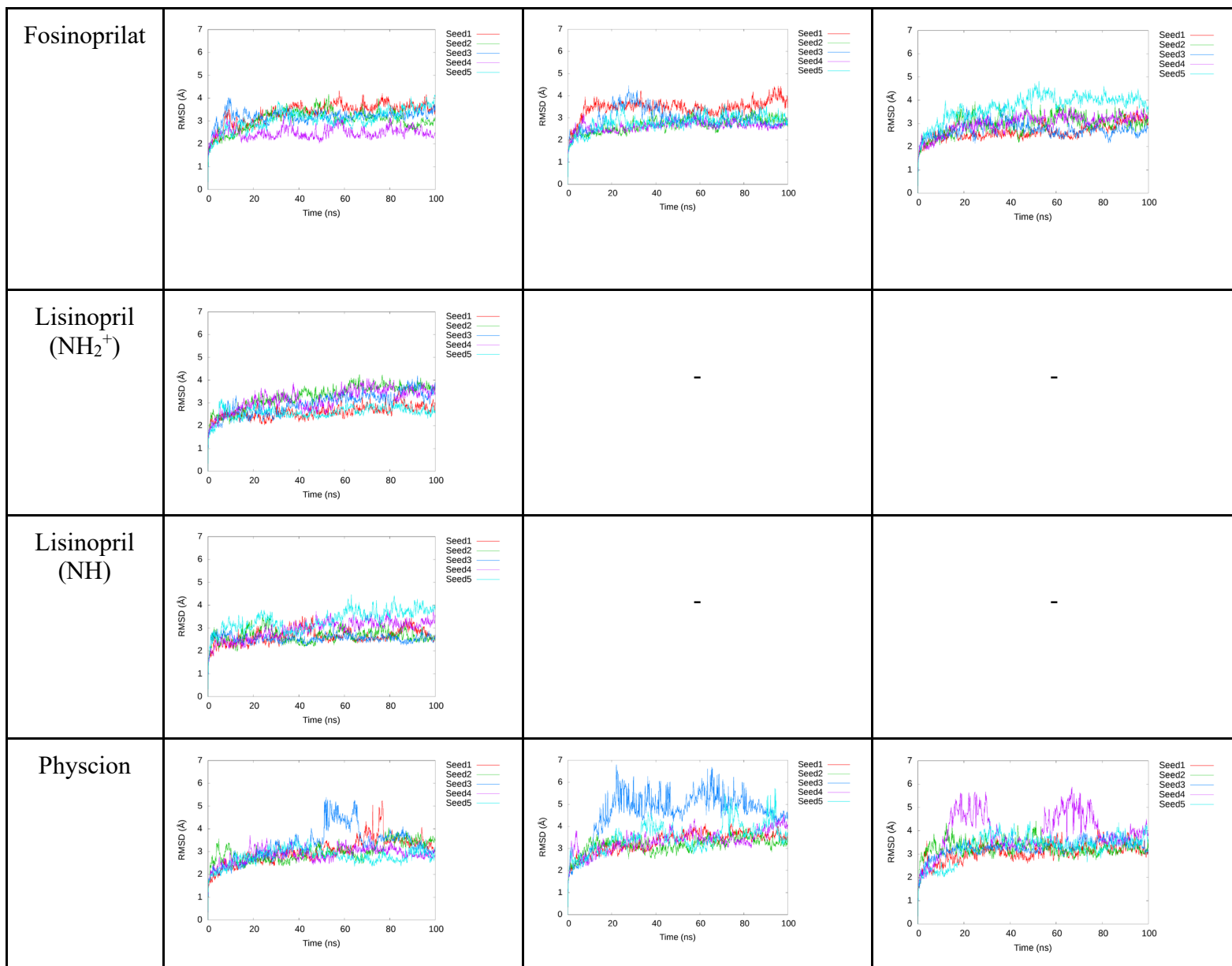
Ligand	Molecular Weight (AMU)	H-Bond Donor	H-Bond Acceptor	logP Octanol/Water	logS Aqueous Solubility	logBB Brain/Blood	logIC ₅₀ HERG K ⁺
Diquafosol	<u>790.311</u>	6.000	<u>33.200</u>	<u>-5.404</u>	0.031	6.000	1.064
Emodin	270.241	1.000	4.250	1.252	-3.051	-1.535	-4.330
Fisinopril	563.670	1.000	12.000	4.677	-5.917	-1.605	-3.374
Fisinoprilat	435.499	1.000	9.000	3.540	-4.264	-1.880	-0.732
Lisinopril (NH₂⁺)	405.493	5.000	9.500	-1.209	-1.142	-1.944	-1.828
Lisinopril (NH)	405.493	5.000	9.500	-1.199	-1.080	-1.494	-1.889
Physcion	284.268	0.00	4.250	1.849	-3.978	-1.045	-4.366

As mentioned in Table S9, diquafosol exceeds the indicated range for the properties: molecular weight, H-bond acceptor, and logP octanol/water. This analysis indicated that diquafosol is water soluble, which is further supported given that it is a common compound in eye drops. Additionally, the molecular structure of diquafosol is notably uncommon with four chained phosphate groups, so it is possible that the ADME program is not trained on molecules of similar structures. The ADME program noted that diquafosol exceeds the molecular weight of the drugs trained for the properties of aqueous solubility and logIC₅₀. Again, this could be due to the distinct structure of the molecule.

Ligand-Bound MD Simulations

Table S10. RMSD for all drug-bound complexes selected for MD simulations.





Analysis of Drugs - Amino Acid Interactions:

Table S11. Hydrogen bonding percent occurrences and pairwise decomposition energies for apo and ligand-bound complexes. Listed below are hydrogen bonding interactions between RBD and hACE2 residues. These interactions have average percent occurrences greater than 5% for at least one of the complexes. Then for each hydrogen bond, the corresponding average pairwise decomposition energy is listed in kcal/mol with the standard deviation. A dash is listed for hydrogen bonds that were not greater than 5% or not present for the specific complex. **A.** For the interaction, RBD Ala475 - hACE2 Ser19 (HX-N), HX-N refers to a hydrogen bond taking place

between residue Ala475 and hydrogens (where X = 1, 2, or 3) on a nitrogen present on the amino acid Ser. This previously mentioned interaction differs from the first RBD Ala475 - hACE2 Ser19 interaction in that the first interaction is between residue Ala475 and oxygen on Ser.

		Apo		Fosinopril Pose 1		Fosinoprilat Pose 2		Fosinoprilat Pose 3		Lisinopril Pose 1	
RBD Residue	hACE2 Residue	Hydrogen Bonding Percent Occurrence (avg.)	Pairwise Decomposition (avg. ± std. dev.) (kcal/mol)	Hydrogen Bonding Percent Occurrence (avg.)	Pairwise Decomposition (avg. ± std. dev.) (kcal/mol)	Hydrogen Bonding Percent Occurrence (avg.)	Pairwise Decomposition (avg. ± std. dev.) (kcal/mol)	Hydrogen Bonding Percent Occurrence (avg.)	Pairwise Decomposition (avg. ± std. dev.) (kcal/mol)	Hydrogen Bonding Percent Occurrence (avg.)	Pairwise Decomposition (avg. ± std. dev.) (kcal/mol)
Asn487	Tyr83	69.56	-2.89 ± 0.96	61.42	-3.11 ± 0.84	46.94	-2.97 ± 0.89	65.66	-2.98 ± 0.88	66.34	-3.13 ± 0.80
	Gln24	19.62	-2.87 ± 0.93	16.20	-2.93 ± 0.87	15.08	-2.79 ± 0.98	20.84	-2.88 ± 0.89	19.08	-2.95 ± 0.89
Gly502	Lys353	66.80	-1.63 ± 0.32	49.88	-1.48 ± 0.34	48.04	-1.57 ± 0.31	60.62	-1.61 ± 0.33	52.70	-1.47 ± 0.31
Tyr449	Asp38	59.72	-3.59 ± 2.01	46.48	-3.33 ± 2.07	56.04	-4.53 ± 1.24	53.06	-3.63 ± 1.95	60.98	-4.06 ± 1.75
	Gln42	-	-0.76 ± 0.92	-	-0.93 ± 1.00	-	-0.81 ± 0.88	7.74	-0.78 ± 1.02	7.70	-0.99 ± 1.02
Lys417	Asp30	57.81	-6.52 ± 2.94	35.32	-4.86 ± 3.76	41.52	-5.62 ± 3.51	53.18	-6.79 ± 3.06	61.14	-9.38 ± 3.50
Gln493	Glu35	52.44	-4.50 ± 1.80	50.08	-4.69 ± 1.55	39.28	-4.54 ± 1.73	55.10	-4.87 ± 1.57	51.26	-4.77 ± 1.60
	Lys31	36.74	-4.13 ± 1.95	28.48	-4.31 ± 1.80	22.80	-3.87 ± 2.06	34.48	-3.80 ± 2.02	30.24	-4.09 ± 2.06
	His34	-	-2.12 ± 1.23	-	-2.32 ± 1.45	8.04	-2.57 ± 1.29	8.80	-2.57 ± 1.28	5.82	-2.10 ± 1.47
Tyr505	Glu37	44.40	-2.86 ± 2.38	33.56	-2.43 ± 2.21	25.54	-2.46 ± 2.28	54.64	-3.55 ± 2.19	61.88	-4.24 ± 1.97
	Arg393	-	-1.42 ± 1.23	-	-0.56 ± 0.63	-	-0.73 ± 0.75	-	-0.72 ± 0.73	7.00	-1.03 ± 1.08

	Ala386	10.08	-0.50 ± 0.82	-	-0.27 ± 0.27	-	-0.33 ± 0.48	-	-0.18 ± 0.15	-	-0.18 ± 0.13
Thr500	Asp355	42.19	-4.70 ± 2.44	47.24	-5.68 ± 2.34	32.80	-5.29 ± 2.32	47.10	-5.30 ± 2.33	54.10	-5.75 ± 2.07
	Tyr41	29.68	-1.26 ± 1.46	17.90	-0.71 ± 1.32	21.38	-1.02 ± 1.38	20.76	-0.95 ± 1.38	14.28	-0.48 ± 1.13
Gln498	Lys353	34.90	-3.86 ± 3.30	-	-0.80 ± 2.19	24.18	-4.14 ± 3.03	45.18	-4.42 ± 3.23	19.08	-1.81 ± 3.13
	Asp38	19.52	-1.68 ± 2.27	-	-0.69 ± 1.44	12.28	-1.95 ± 2.37	27.72	-2.13 ± 2.27	-	-0.68 ± 1.45
	Gln42	-	-0.41 ± 1.12	11.18	-1.18 ± 1.49	-	-0.34 ± 1.20	-	-0.17 ± 0.68	-	-0.47 ± 1.15
Gly496	Lys353	26.47	-3.25 ± 1.77	6.80	-2.23 ± 1.50	18.56	-3.46 ± 1.62	18.56	-3.38 ± 1.47	7.12	-2.40 ± 1.57
Tyr453	His34	24.98	-2.07 ± 1.05	16.92	-1.76 ± 1.16	35.28	-2.38 ± 1.16	33.30	-2.48 ± 1.21	10.32	-1.33 ± 0.86
Ala475	Ser19	17.37	-0.73 ± 1.29	28.22	-1.35 ± 1.35	17.48	-1.53 ± 1.51	26.48	-1.54 ± 1.39	15.64	-1.49 ± 1.61
	Gln24	11.76	-1.93 ± 1.18	-	-1.52 ± 0.88	7.60	-1.71 ± 1.03	-	-1.52 ± 1.00	9.80	-1.71 ± 1.05
	Ser19 (HX-N)	-	0.73 ± 1.29	-	-1.35 ± 1.35	6.60	-1.53 ± 1.51	-	-1.54 ± 1.39	5.38	-1.49 ± 1.61
Ser494	His34	9.93	-1.05 ± 1.07	-	-0.23 ± 0.28	-	-0.40 ± 0.64	-	-0.43 ± 0.71	-	-0.32 ± 0.45
Gly446	Gln42	9.02	-0.71 ± 0.97	7.06	-0.96 ± 1.01	8.42	-0.92 ± 1.11	13.20	-0.74 ± 1.10	13.60	-0.98 ± 1.14
Tyr495	Lys353	7.75	-0.31 ± 2.00	16.00	-1.44 ± 2.39	5.54	-0.96 ± 2.34	13.44	-0.81 ± 2.33	17.78	-2.04 ± 2.27
Tyr489	Tyr83	-	-0.11 ± 0.38	7.10	-0.24 ± 0.63	-	-0.10 ± 0.33	-	-0.40 ± 0.20	10.46	-0.33 ± 0.69

Table S12. Average pairwise decomposition energies for interactions involving fosinopril. Additionally, the average van der Waals and electrostatic energies are included, as well as the standard deviation and standard error for all energies. All values are reported in units of kcal/mol. Interactions were selected if pairwise decomposition was less than -1 kcal/mol.

Residue	van der Waals Avg. ± Std. Dev. (Std. Error)	Electrostatic Avg. ± Std. Dev. (Std. Error)	Pairwise Decomposition Avg. ± Std. Dev. (Std. Error)
RBD Arg408	-0.36 ± 0.94 (0.04)	-38.32 ± 16.85 (0.75)	-8.27 ± 5.82 (0.26)
RBD Arg403	-0.95 ± 1.10 (0.05)	-24.51 ± 11.76 (0.53)	-7.17 ± 6.01 (0.27)
hACE2 His34	-1.60 ± 1.34 (0.06)	-0.67 ± 0.79 (0.04)	-2.95 ± 2.38 (0.11)
hACE2 Ala387	-1.39 ± 0.68 (0.03)	-0.14 ± 0.82 (0.04)	-2.66 ± 1.25 (0.06)
hACE2 Pro389	-0.97 ± 0.69 (0.03)	-0.19 ± 0.34 (0.02)	-1.87 ± 1.36 (0.06)
hACE2 Arg559	-0.53 ± 0.90 (0.04)	-14.58 ± 8.97 (0.40)	-1.73 ± 3.33 (0.15)
hACE2 Gln388	-0.93 ± 0.79 (0.04)	-0.09 ± 0.95 (0.04)	-1.52 ± 1.41 (0.06)
RBD Tyr505	-0.89 ± 0.75 (0.03)	0.25 ± 0.54 (0.02)	-1.50 ± 1.38 (0.06)
RBD Lys417	-0.72 ± 0.73 (0.03)	-13.96 ± 5.05 (0.23)	-1.42 ± 1.41 (0.06)
hACE2 Asn33	-0.64 ± 0.52 (0.02)	-0.14 ± 0.44 (0.02)	-1.19 ± 0.98 (0.04)

Table S13. Average pairwise decomposition energies for interactions involving fosinoprilat pose 2. Additionally, the average van der Waals and electrostatic energies are included, as well as the standard deviation and standard error for all energies. All values are reported in units of kcal/mol. Interactions were selected if pairwise decomposition was less than -1 kcal/mol.

Residue	van der Waals Avg. ± Std. Dev. (Std. Error)	Electrostatic Avg. ± Std. Dev. (Std. Error)	Pairwise Decomposition Avg. ± Std. Dev. (Std. Error)
RBD Arg403	-1.03 ± 0.90 (0.04)	-59.07 ± 13.69 (0.61)	-14.92 ± 7.99 (0.36)
RBD Arg408	-0.66 ± 1.24 (0.06)	-55.46 ± 14.84 (0.66)	-8.20 ± 6.84 (0.31)
RBD Lys417	-0.25 ± 0.48 (0.02)	-52.90 ± 17.06 (0.76)	-5.37 ± 6.67 (0.30)
hACE2 His34	-2.24 ± 0.66 (0.03)	-3.80 ± 4.26 (0.19)	-4.42 ± 2.31 (0.10)
hACE2 Lys353	-0.63 ± 0.40 (0.02)	-26.31 ± 2.97 (0.13)	-2.52 ± 1.66 (0.07)
RBD Tyr505	-1.12 ± 0.49 (0.02)	0.24 ± 1.76 (0.08)	-1.89 ± 1.06 (0.05)
hACE2 Asn33	-0.76 ± 0.47 (0.02)	-2.15 ± 1.98 (0.09)	-1.79 ± 1.56 (0.07)

hACE2 Gln388	-0.89 ± 0.74 (0.03)	2.11 ± 1.51 (0.07)	-1.72 ± 1.41 (0.06)
hACE2 Pro389	-1.01 ± 0.71 (0.03)	-1.91 ± 1.13 (0.05)	-1.71 ± 1.49 (0.07)
hACE2 Ala387	-0.90 ± 0.62 (0.03)	2.95 ± 1.15 (0.05)	-1.65 ± 1.19 (0.05)
hACE2 Glu37	-1.07 ± 0.37 (0.02)	31.06 ± 3.44 (0.15)	-1.65 ± 0.69 (0.03)
hACE2 Arg393	-0.36 ± 0.23 (0.01)	-35.61 ± 5.64 (0.25)	-1.56 ± 1.87 (0.08)
Glycan	-0.65 ± 0.67 (0.03)	-6.74 ± 2.96 (0.13)	-1.41 ± 1.71 (0.08)
RBD Tyr495	-0.58 ± 0.30 (0.01)	-1.49 ± 0.76 (0.03)	-1.01 ± 0.46 (0.02)

Table S14. Average pairwise decomposition energies for interactions involving fosinoprilat pose 3. Additionally, the average van der Waals and electrostatic energies are included, as well as the standard deviation and standard error for all energies. All values are reported in units of kcal/mol. Interactions were selected if pairwise decomposition was less than -1 kcal/mol.

Residue	van der Waals Avg. ± Std. Dev. (Std. Error)	Electrostatic Avg. ± Std. Dev. (Std. Error))	Pairwise Decomposition Avg. ± Std. Dev. (Std. Error)
RBD Arg408	-0.14 ± 1.05 (0.05)	-64.27 ± 17.25 (0.77)	-11.11 ± 7.99 (0.36)
RBD Arg403	-1.03 ± 0.83 (0.04)	-45.75 ± 15.27 (0.68)	-7.28 ± 7.42 (0.33)
RBD Lys417	-0.35 ± 0.47 (0.02)	-46.87 ± 15.89 (0.71)	-4.43 ± 6.42 (0.29)
hACE2 His34	-1.34 ± 1.04 (0.05)	-4.93 ± 4.71 (0.21)	-3.86 ± 3.16 (0.14)
Glycan	-0.76 ± 0.74 (0.03)	-8.61 ± 7.00 (0.31)	-3.25 ± 4.83 (0.22)
hACE2 Pro389	-1.20 ± 0.85 (0.04)	-1.35 ± 0.60 (0.03)	-2.11 ± 1.54 (0.07)
hACE2 Ala387	-0.93 ± 0.67 (0.03)	1.78 ± 1.10 (0.05)	-1.74 ± 1.26 (0.06)
hACE2 Asn33	-0.74 ± 0.42 (0.02)	-1.58 ± 1.65 (0.07)	-1.66 ± 0.91 (0.04)
hACE2 Gln388	-0.91 ± 0.69 (0.03)	1.33 ± 1.28 (0.06)	-1.66 ± 1.32 (0.06)
hACE2 Lys26	-0.07 ± 0.26 (0.01)	-29.26 ± 12.81 (0.57)	-1.50 ± 4.23 (0.19)
hACE2 Arg393	-0.41 ± 0.29 (0.01)	-30.21 ± 4.10 (0.18)	-1.43 ± 1.11 (0.05)
RBD Gln409	-0.33 ± 0.40 (0.02)	-4.01 ± 2.53 (0.11)	-1.21 ± 1.47 (0.07)

RBD Tyr505	-0.75 ± 0.64 (0.03)	0.61 ± 0.71 (0.03)	-1.11 ± 0.97 (0.04)
------------	---------------------	--------------------	---------------------

Table S15. Average pairwise decomposition energies for interactions involving lisinopril. Additionally, the average van der Waals and electrostatic energies are included, as well as the standard deviation and standard error for all energies. All values are reported in units of kcal/mol. Interactions were selected if pairwise decomposition was less than -1 kcal/mol.

Residue	van der Waals Avg. ± Std. Dev. (Std. Error)	Electrostatic Avg. ± Std. Dev. (Std. Error)	Pairwise Decomposition Avg. ± Std. Dev. (Std. Error)
RBD Arg408	-0.13 ± 0.78 (0.03)	-35.15 ± 13.91 (0.62)	-6.96 ± 5.97 (0.27)
RBD Lys417	-0.44 ± 0.58 (0.03)	-27.15 ± 12.77 (0.57)	-5.29 ± 5.98 (0.27)
hACE2 Asp30	-1.84 ± 1.30 (0.06)	15.91 ± 7.43 (0.33)	-4.46 ± 4.63 (021)
hACE2 His34	-2.03 ± 1.38 (0.06)	-2.71 ± 2.46 (0.11)	-4.12 ± 3.07 (0.14)
hACE2 Asn33	-1.96 ± 1.08 (0.05)	-0.97 ± 1.97 (0.09)	-3.50 ± 2.69 (0.12)
hACE2 Glu37	-0.74 ± 0.91 (0.04)	10.43 ± 3.15 (0.14)	-2.78 ± 3.57 (0.16)
hACE2 Pro389	-1.52 ± 0.74 (0.03)	-0.48 ± 0.51 (0.02)	-2.50 ± 1.10 (0.05)
Glycan	-1.02 ± 0.61 (0.03)	-3.69 ± 1.46 (0.07)	-2.16 ± 1.35 (0.06)
RBD Arg403	-0.79 ± 0.50 (0.02)	-18.09 ± 4.42 (0.20)	-2.00 ± 1.59 (0.07)
hACE2 Leu29	-0.81 ± 0.55 (0.02)	-0.24 ± 0.44 (0.02)	-1.62 ± 1.12 (0.05)
hACE2 Lys26	-0.73 ± 0.59 (0.03)	-13.19 ± 2.69 (0.12)	-1.62 ± 1.35 (0.06)
hACE2 Gln388	-0.82 ± 0.85 (0.04)	0.46 ± 1.09 (0.05)	-1.52 ± 1.63 (0.07)
hACE2 Ala387	-0.80 ± 0.82 (0.04)	1.34 ± 1.02 (0.05)	-1.47 ± 1.62 (0.07)
hACE2 Gln96	-0.45 ± 0.38 (0.02)	-1.03 ± 1.36 (0.06)	-1.45 ± 1.45 (0.06)
RBD Asp405	-0.70 ± 0.44 (0.02)	19.04 ± 4.23 (0.19)	-1.05 ± 1.01 (0.05)

Fosinopril

Table S16. SARS-CoV-2 RBD - hACE2 fosinopril pairwise decomposition energies. Listed in the table are the average pairwise decomposition energies for interactions between RBD and

hACE2 residues when fosinopril is present in the interface. Additionally, the average van der Waals and electrostatic energies are included, as well as the standard deviation and standard error for all energies. All values are reported in units of kcal/mol. Interactions were selected if pairwise decomposition was less than -2 kcal/mol.

RBD Residue	hACE2 Residue	van der Waals Avg. ± Std. Dev. (Std. Error)	Electrostatic Avg. ± Std. Dev. (Std. Error)	Pairwise Decomposition Avg. ± Std. Dev. (Std. Error)
Thr500	Asp355	-0.54 ± 0.60 (0.03)	-4.48 ± 3.03 (0.14)	-5.68 ± 2.34 (0.10)
Asn501	Lys353	-1.52 ± 0.31 (0.01)	-3.72 ± 1.79 (0.08)	-5.06 ± 1.20 (0.05)
Tyr505	Lys353	-2.16 ± 0.39 (0.02)	-1.39 ± 0.76 (0.03)	-4.94 ± 0.55 (0.02)
Lys417	Asp30	0.12 ± 0.61 (0.03)	-38.31 ± 10.10 (0.45)	-4.86 ± 3.76 (0.17)
Gln493	Glu35	-0.44 ± 0.57 (0.03)	-5.03 ± 2.36 (0.11)	-4.69 ± 1.55 (0.07)
Gln493	Lys31	-0.21 ± 0.52 (0.02)	-7.48 ± 2.53 (0.11)	-4.31 ± 1.80 (0.08)
Tyr449	Asp38	0.10 ± 0.77 (0.03)	-5.72 ± 4.19 (0.19)	-3.33 ± 2.07 (0.09)
Asn487	Tyr83	0.02 ± 0.62 (0.03)	-3.72 ± 1.21 (0.05)	-3.11 ± 0.84 (0.04)
Asn487	Gln24	-0.91 ± 0.40 (0.02)	-1.33 ± 1.26 (0.06)	-2.93 ± 0.87 (0.04)
Phe486	Met82	-1.27 ± 0.41 (0.02)	-0.04 ± 0.27 (0.01)	-2.59 ± 0.77 (0.03)
Tyr505	Glu37	-0.19 ± 0.54 (0.02)	-4.30 ± 3.80 (0.17)	-2.43 ± 2.21 (0.10)
Gln493	His34	-0.91 ± 0.31 (0.01)	-1.82 ± 1.24 (0.06)	-2.32 ± 1.45 (0.06)
Gly496	Lys353	-0.21 ± 0.43 (0.02)	-3.81 ± 3.03 (0.14)	-2.23 ± 1.50 (0.07)
Gln498	Tyr41	-1.02 ± 0.37 (0.02)	-0.05 ± 0.59 (0.03)	-2.21 ± 0.70 (0.03)
Asn501	Tyr41	-0.66 ± 0.30 (0.01)	-0.42 ± 0.63 (0.03)	-2.01 ± 1.03 (0.05)

Table S17. Hydrogen bonds and percent occurrence for fosinopril. Hydrogen bonds involving fosinopril with a percent occurrence greater than 5% are listed.

Acceptor	Donor	Hydrogen Bonding Percent Occurrence (avg.)
Fosinopril @ O2	RBD - Arg403 @ HH12-NH1, HH22-NH2	54.94
Fosinopril @ O6	RBD - Arg408 @ HH11-NH1, HH12-NH1, HH21-NH2, HH22-NH2	22.84
Fosinopril @ O7	RBD - Arg408 @ HH11-NH1, HH12-NH1, HH21-NH2, HH22-NH2	21.84
Fosinopril @ O5	RBD - Gln409 @ HE22-NE2	8.64
Fosinopril @ O7	RBD - Arg408 @ HE-NE	8.42
Fosinopril @ O6	RBD - Arg408 @ HE-NE	8.06
Fosinopril @ O1	RBD - Arg408 @ HH11-NH1, HH12-NH1, HH22-NH2	8.06

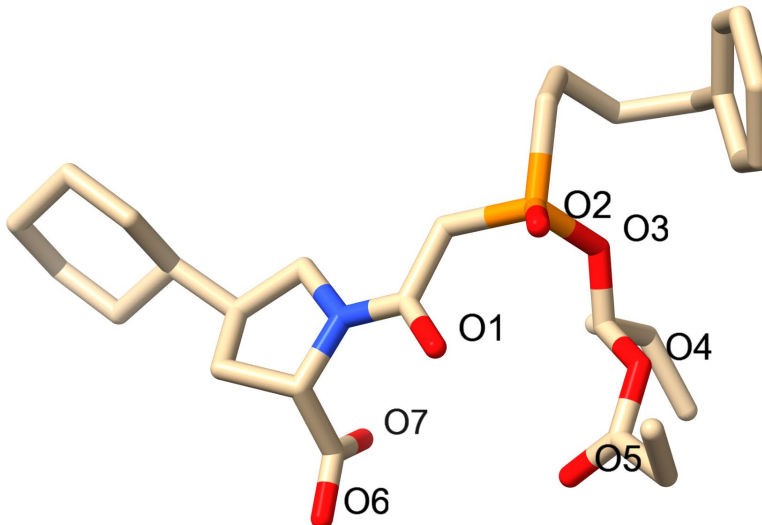


Figure S6. Fosinopril with oxygen labels.

Based on hydrogen bonding analysis, fosinopril disrupts the interactions RBD Ala475 - hACE2 Gln24, RBD Gln498 - hACE2 Lys353, and RBD Gln498 - hACE2 Asp38. The disruption of the interactions RBD Gln498 - hACE2 Lys353 and RBD Gln498 - hACE2 Asp38 are further supported by the increase in pairwise decomposition energy of these interactions. Also, a notable electrostatic interaction occurs between hACE2 Lys353 and fosinopril with an average electrostatic energy of -10.01 (0.09) kcal/mol and an average pairwise decomposition energy of -0.64 (0.05) kcal/mol, further supporting that the presence of fosinopril in the interface disrupts the interaction between RBD Gln498 and hACE2 Lys353. There is a prominent decrease (difference greater than 15%) in the hydrogen bond occurrence for the following interactions when fosinopril is present in the interface: RBD Gly502 - hACE2 Lys353, RBD Lys417 - hACE2 Asp30, and RBD Gly496 - hACE2 Lys353. Notably, Lys417 and fosinopril form a significant electrostatic interaction with an average electrostatic energy of -13.96 (0.23) kcal/mol and an average pairwise decomposition energy of -1.42 (0.06) kcal/mol.

Table S16 contains the pairwise decomposition energies for interactions between the RBD and hACE2 with energies less than -2 kcal/mol when fosinopril is bound in the interface. There is a notable decrease in the average pairwise decomposition energy of the interactions RBD Gln498 - hACE2 Gln42 and RBD Thr500 - hACE2 Asp355 when fosinopril is present. There is an increase in the hydrogen bond occurrence of the interaction RBD Gln498 - hACE2 Gln42. This information suggests that the presence of fosinopril in the interface enhances these two interactions, demonstrating that the drug not only inhibits but, to a lesser degree, strengthens the interaction between the RBD and hACE2.

Table S17 contains the hydrogen bonding interactions involving fosinopril. It is important to note that three significant hydrogen bonds between oxygen atoms on fosinopril and RBD residues, such as Arg403 and Arg408, have a percent occurrence above 20%. Additionally, the average pairwise decomposition energies of the interaction between the RBD residues Arg403 and Arg408 with fosinopril are -7.17 (0.27) and -8.27 (0.26) kcal/mol, respectively. Interestingly, the significant hydrogen bonding interactions that form between fosinopril and the RBD do not involve RBD residues that are present in the previously mentioned disrupted, diminished, or enhanced interactions. The formation of these interactions, along with other electrostatic or van der Waals interactions, cause the previous interactions to be unfavorable or more favorable.

Fosinoprilat

Table S18. Hydrogen bonds and percent occurrence for fosinoprilat pose 2. Hydrogen bonds involving fosinoprilat in pose 2 with a percent occurrence greater than 5% are listed.

Acceptor	Donor	Hydrogen Bonding Percent Occurrence (avg.)
Fosinoprilat @ O5	RBD - Arg408 @ HH11-NH1, HH12-NH1, HH22-NH2	22.36
Fosinoprilat @ O3	RBD - Arg403 @ HH12-NH1, HH22-NH2	22.00
Fosinoprilat @ O2	RBD - Arg403 @ HH12-NH1, HH22-NH2	20.88
Fosinoprilat @ O4	RBD - Arg408 @ HH11-NH1, HH12-NH1, HH22-NH2	20.60
Fosinoprilat @ O2	RBD - Lys417 @ HZ1, HZ2, HZ3-NZ	11.44

Table S19. SARS-CoV-2 RBD - hACE2 fosinoprilat pose 2 pairwise decomposition energies. Listed in the table are the average pairwise decomposition energies for interactions between RBD and hACE2 residues when fosinoprilat in pose 2 is present in the interface. Additionally, the average van der Waals and electrostatic energies are included, as well as the standard deviation and standard error for all energies. All values are reported in units of kcal/mol. Interactions were selected if pairwise decomposition was less than -2 kcal/mol.

RBD Residue	hACE2 Residue	van der Waals Avg. ± Std. Dev. (Std. Error)	Electrostatic Avg. ± Std. Dev. (Std. Error)	Pairwise Decomposition Avg. ± Std. Dev. (Std. Error)
Lys417	Asp30	0.11 ± 0.64 (0.03)	-41.11 ± 9.36 (0.42)	-5.62 ± 3.51 (0.16)
Thr500	Asp355	-0.63 ± 0.64 (0.03)	-3.74 ± 3.03 (0.14)	-5.29 ± 2.32 (0.10)
Tyr505	Lys353	-2.06 ± 0.38 (0.02)	-1.68 ± 0.77 (0.03)	-4.78 ± 0.60 (0.03)
Asn501	Lys353	-1.60 ± 0.30 (0.01)	-3.60 ± 1.67 (0.07)	-4.61 ± 1.24 (0.06)
Gln493	Glu35	-0.43 ± 0.60 (0.03)	-4.75 ± 2.61 (0.12)	-4.54 ± 1.73 (0.08)
Tyr449	Asp38	0.31 ± 0.70 (0.03)	-8.25 ± 2.15 (0.10)	-4.53 ± 1.24 (0.06)
Gln498	Lys353	-0.18 ± 0.46 (0.02)	-5.42 ± 4.37 (0.20)	-4.14 ± 3.03 (0.14)

Gln493	Lys31	-0.19 ± 0.45 (0.02)	-6.88 ± 3.06 (0.14)	-3.87 ± 2.06 (0.09)
Gly496	Lys353	0.07 ± 0.55 (0.02)	-5.52 ± 2.23 (0.10)	-3.46 ± 1.62 (0.07)
Asn487	Tyr83	-0.07 ± 0.53 (0.02)	-3.35 ± 1.47 (0.07)	-2.97 ± 0.89 (0.04)
Asn487	Gln24	-0.88 ± 0.41 (0.02)	-1.36 ± 1.23 (0.05)	-2.80 ± 0.98 (0.04)
Phe486	Met82	-1.30 ± 0.38 (0.01)	-0.008 ± 0.270 (0.012)	-2.57 ± 0.68 (0.03)
Gln493	His34	-0.85 ± 0.44 (0.02)	-1.90 ± 1.45 (0.06)	-2.57 ± 1.29 (0.06)
Tyr505	Glu37	-0.29 ± 0.51 (0.02)	-3.73 ± 3.98 (0.18)	-2.46 ± 2.28 (0.10)
Tyr453	His34	-0.30 ± 0.55 (0.02)	-2.19 ± 1.38 (0.06)	-2.38 ± 1.16 (0.05)
Asn501	Tyr41	-0.74 ± 0.25 (0.01)	-0.59 ± 0.63 (0.03)	-2.37 ± 1.03 (0.05)
Phe486	Tyr83	-0.99 ± 0.38 (0.02)	-0.39 ± 0.25 (0.01)	-2.09 ± 0.65 (0.03)

Table S20. Hydrogen bonds and percent occurrence for fosinoprilat pose 3. Hydrogen bonds involving fosinoprilat in pose 3 with a percent occurrence greater than 5% are listed.

Acceptor	Donor	Hydrogen Bonding Percent Occurrence (avg.)
Fosinoprilat @ O4	RBD - Arg408 @ HH11-NH1, HH12-NH1, HH21-NH2, HH22-NH2	21.08
Fosinoprilat @ O5	RBD - Arg408 @ HH11-NH1, HH12-NH1, HH21-NH2, HH22-NH2	19.90
Fosinoprilat @ O2	hACE2 His34 @ HE2-NE2	18.14
Fosinoprilat @ O3	RBD - Arg408 @ HH11-NH1, HH12-NH1, HH22-NH2	17.84
Fosinoprilat @ O2	RBD - Arg408 @ HH11-NH1, HH12-NH1, HH22-NH2	13.52

Fosinoprilat @ O3	RBD - Arg403 @ HH12-NH1, HH21-NH2, HH22-NH2	12.84
Fosinoprilat @ O2	RBD - Lys417 @ HZ1, HZ2, HZ3-NZ	9.20
Fosinoprilat @ O2	hACE2 - Glycan @ H4O-O4	8.32
Fosinoprilat @ O2	hACE2 - Glycan @ H3O-O3	8.00
Fosinoprilat @ O3	hACE2 - Lys26 @ HZ1, HZ2, HZ3-NZ	5.46
Fosinoprilat @ O3	RBD - Lys417 @ HZ1, HZ2, HZ3-NZ	5.38
Fosinoprilat @ O1	RBD - Arg408 @ HH11-NH1, HH12-NH1, HH22-NH2	5.20

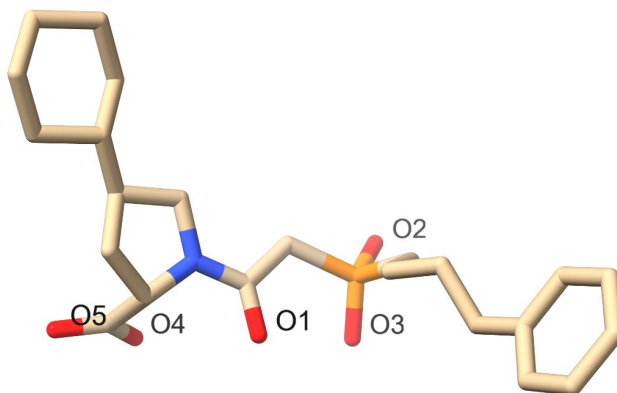


Figure S7. Fosinoprilat with oxygen labels.

Table S21. SARS-CoV-2 RBD - hACE2 fosinoprilat pose 3 pairwise decomposition Energies. Listed in the table are the average pairwise decomposition energies for interactions between RBD and hACE2 residues when fosinoprilat in pose 3 is present in the interface. Additionally, the average van der Waals and electrostatic energies are included, as well as the standard deviation and standard error for all energies. All values are reported in units of kcal/mol. Interactions were selected if pairwise decomposition was less than -2 kcal/mol.

RBD Residue	hACE2 Residue	van der Waals Avg. ± Std. Dev. (Std. Error)	Electrostatic Avg. ± Std. Dev. (Std. Error)	Pairwise Decomposition Avg. ± Std. Dev. (Std. Error)
Lys417	Asp30	0.12 ± 0.62 (0.03)	-43.65 ± 7.77 (0.35)	-6.79 ± 3.06 (0.14)
Thr500	Asp355	-0.65 ± 0.60 (0.03)	-3.80 ± 3.05 (0.14)	-5.30 ± 2.33 (0.10)
Tyr505	Lys353	-2.24 ± 0.33 (0.01)	-1.51 ± 0.79 (0.04)	-5.08 ± 0.52 (0.02)
Asn501	Lys353	-1.64 ± 0.28 (0.01)	-4.15 ± 1.71 (0.08)	-5.08 ± 1.36 (0.06)
Gln493	Glu35	-0.43 ± 0.61 (0.03)	-5.16 ± 2.43 (0.11)	-4.87 ± 1.57 (0.07)
Gln498	Lys353	-0.17 ± 0.48 (0.02)	-5.35 ± 4.80 (0.21)	-4.42 ± 3.23 (0.14)
Gln493	Lys31	-0.15 ± 0.53 (0.02)	-6.77 ± 3.24 (0.14)	-3.80 ± 2.02 (0.09)
Tyr449	Asp38	0.09 ± 0.70 (0.03)	-6.39 ± 3.82 (0.17)	-3.63 ± 1.95 (0.09)
Tyr505	Glu37	-0.16 ± 0.71 (0.03)	-5.69 ± 3.76 (0.17)	-3.55 ± 2.19 (0.10)
Gly496	Lys353	0.09 ± 0.53 (0.02)	-5.37 ± 2.29 (0.10)	-3.38 ± 1.47 (0.07)
Asn487	Tyr83	-0.05 ± 0.53 (0.02)	-3.53 ± 1.25 (0.06)	-2.97 ± 0.88 (0.04)
Asn487	Gln24	-0.89 ± 0.37 (0.02)	-1.43 ± 1.13 (0.05)	-2.88 ± 0.89 (0.04)
Gln493	His34	-0.82 ± 0.43 (0.02)	-1.93 ± 1.52 (0.07)	-2.57 ± 1.28 (0.06)
Tyr453	His34	-0.32 ± 0.57 (0.03)	-2.10 ± 1.57 (0.07)	-2.48 ± 1.21 (0.05)
Phe486	Met82	-1.20 ± 0.41 (0.02)	0.02 ± 0.28 (0.01)	-2.41 ± 0.73 (0.03)
Asn501	Tyr41	-0.73 ± 0.29 (0.01)	-0.51 ± 0.60 (0.03)	-2.21 ± 1.03 (0.05)
Gln498	Asp38	-0.09 ± 0.31 (0.01)	-2.95 ± 2.47 (0.11)	-2.13 ± 2.27 (0.10)

Fosinoprilat pose 2 reduces the occurrence of hydrogen bonds, such as RBD Gly502 - hACE2 Lys353, RBD Lys417 - hACE2 Asp30, RBD Asn487 - hACE2 Tyr83, and RBD Tyr505 - hACE2 Glu37, as shown by Table S11. This decrease in hydrogen bond occurrence could be due to the formation of additional interactions between fosinoprilat (pose 2) and the complex. These interactions are detailed in Tables S13 and S18. Notably, the interaction between fosinoprilat (pose 2) and RBD Lys417 can explain the decrease in the percent occurrence of the hydrogen bond between RBD Lys417 and hACE2 Asp30. Specifically, fosinoprilat (pose 2) competes with this interaction by forming a significant hydrogen bond with RBD Lys417. The average pairwise decomposition energy of the interaction between fosinoprilat (pose 2) and RBD

Lys417 is -5.37 (0.30) kcal/mol. Pairwise decomposition analysis supports the decrease in the hydrogen bond occurrence of RBD Gly502 - hACE2 Lys353 and RBD Tyr505 - hACE2 Glu37. Table S13 demonstrates that fosinoprilat (pose 2) forms a significant electrostatic interaction with hACE2 Lys353 and forms significant van der Waals interactions with RBD Tyr505 and hACE2 Glu37. The average pairwise decomposition energies for the residues hACE2 Lys353, RBD Tyr505, and hACE2 Glu37 interaction with fosinoprilat (pose 2) are -2.52 (0.07), -1.89 (0.05), and -1.65 (0.03) kcal/mol, respectively.

Also, fosinoprilat (pose 2) forms significant hydrogen bonds with the RBD residues Arg408 and Arg403; despite this, these RBD residues are not involved in diminished hydrogen bonding interactions. However, these interactions are significant for fosinoprilat (pose 2) to maintain in the interface, given that the average pairwise decomposition energies of the interaction between the fosinoprilat (pose 2) and the RBD residues Arg408 or Arg403 are -8.20 (0.31) and -14.92 (0.36) kcal/mol. Table S19 contains the average pairwise decomposition energies for interactions between the RBD and hACE2 with energies less than -2 kcal/mol when fosinoprilat (pose 2) is bound. The only notable increase in the average pairwise decomposition energy was for the interaction RBD Tyr449 - hACE2 Asp38 due to a notable decrease in the average electrostatic energy.

The interaction RBD Ala475 - hACE2 Gln24 is disrupted by fosinoprilat pose 3. Fosinoprilat pose 3 does not decrease the occurrence of hydrogen bonds significant for the RBD - hACE2 interaction; however, Table S20 contains hydrogen bonding interactions between fosinoprilat (pose 3) and the complex with an occurrence above 5%. Most hydrogen bonds involve RBD residues Arg403, Arg408, and Lys417. RBD Arg408 is involved in 5 hydrogen bonds with fosinoprilat (pose 3), and the average pairwise decomposition energy of these interactions is -11.11 (0.36) kcal/mol. This suggests that these interactions are significant for fosinoprilat (pose 3) to maintain its position in the interface. Notably, the phosphate oxygen atoms (O3 and O2) on fosinoprilat (pose 3) can compete with hACE2 Asp30, which participates in a significant hydrogen bond with RBD Lys417. The average pairwise decomposition energies between fosinoprilat (pose 3) and Lys417 and between RBD Lys417 and hACE2 Asp30 are -4.43 (0.29) and -6.79 (0.14) kcal/mol, respectively (Figure SCC and Figure 4). Table S21 contains the average pairwise decomposition energies for interactions between the RBD and hACE2 with energies less than -2 kcal/mol when fosinoprilat (pose 3) is bound. Notably, there is an increase in the hydrogen bond occurrences and the average pairwise decomposition energies of the interactions RBD Tyr505 - hACE2 Glu37 and RBD 498 - hACE2 Lys353 when fosinoprilat (pose 3) is bound in the interface.

Lisinopril

Table S22. Hydrogen Bonds and Percent Occurrence for Lisinopril. Hydrogen bonds involving lisinopril with a percent occurrence greater than 5% are listed.

Acceptor	Donor	Hydrogen Bonding Percent Occurrence (avg.)
Lisinopril @ O4	RBD - Arg408 @ HH11-NH1, HH12-NH1, HH22-NH2	28.16
Lisinopril @ O5	RBD - Arg408 @ HH11-NH1, HH12-NH1, HH22-NH2	25.80
hACE2 Glu37 @ OE1, OE2	Lisinopril @ H21, H22, H23-N2	28.58
hACE2 Asp30 @ OD1, OD2	Lisinopril @ H21, H22, H23-N2	26.72
hACE2 Asn33 @ O	Lisinopril @ H21, H22, H23-N2	24.68
Lisinopril @ O5	Lisinopril @ H4-N1	20..24
Lisinopril @ O4	Lisinopril @ H4-N1	16.64
hACE2 Asp30 @ O	Lisinopril @ H21, H22, H23-N2	16.34
Lisinopril @ O1	hACE2 Gln96 @ HE22-NE2	5.70

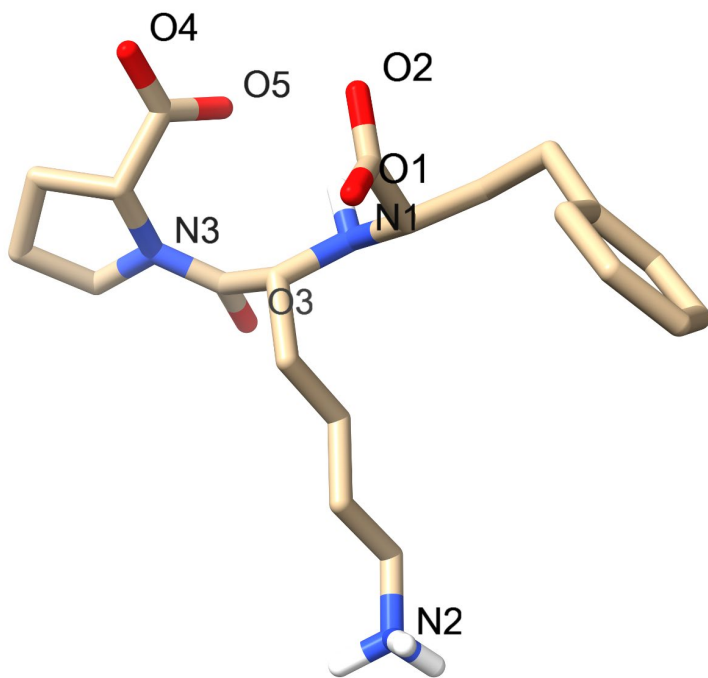


Figure S8. Lisinopril with oxygen and nitrogen labels.

Table S23. SARS-CoV-2 RBD - hACE2 lisinopril pairwise decomposition energies. Listed in the table are the average pairwise decomposition energies for interactions between RBD and hACE2 residues when lisinopril is present in the interface. Additionally, the average van der Waals and electrostatic energies are included, as well as the standard deviation and standard error for all energies. All values are reported in units of kcal/mol. Interactions were selected if pairwise decomposition was less than -2 kcal/mol.

RBD Residue	hACE2 Residue	van der Waals Avg. ± Std. Dev. (Std. Error)	Electrostatic Avg. ± Std. Dev. (Std. Error)	Pairwise Decomposition Avg. ± Std. Dev. (Std. Error)
Lys417	Asp30	0.39 ± 0.74 (0.03)	-48.71 ± 7.44 (0.33)	-9.38 ± 3.50 (0.16)
Thr500	Asp355	-0.49 ± 0.65 (0.03)	-4.59 ± 2.65 (0.12)	-5.75 ± 2.07 (0.09)
Tyr505	Lys353	-2.19 ± 0.37 (0.02)	-1.11 ± 0.75 (0.03)	-5.06 ± 0.46 (0.02)
Asn501	Lys353	-1.52 ± 0.32 (0.01)	-3.48 ± 1.75 (0.08)	-4.92 ± 1.04 (0.05)
Gln493	Glu35	-0.50 ± 0.58 (0.03)	-5.15 ± 2.45 (0.11)	-4.77 ± 1.60 (0.07)
Tyr505	Glu37	0.03 ± 0.74 (0.03)	-6.93 ± 3.34 (0.15)	-4.24 ± 1.97 (0.09)
Gln493	Lys31	-0.17 ± 0.52 (0.02)	-7.04 ± 2.95 (0.13)	-4.09 ± 2.06 (0.09)
Tyr449	Asp38	0.14 ± 0.73 (0.03)	-7.08 ± 3.55 (0.16)	-4.06 ± 1.75 (0.08)
Asn487	Tyr83	-0.07 ± 0.55 (0.02)	-3.63 ± 1.28 (0.06)	-3.13 ± 0.80 (0.04)
Asn487	Gln24	-0.90 ± 0.38 (0.02)	-1.39 ± 1.29 (0.06)	-2.95 ± 0.89 (0.04)
Phe486	Met82	-1.32 ± 0.43 (0.02)	0.001 ± 0.289 (0.013)	-2.64 ± 0.76 (0.03)
Gly496	Lys353	-0.18 ± 0.42 (0.02)	-4.29 ± 2.46 (0.11)	-2.40 ± 1.57 (0.07)
Gln498	Tyr41	-1.03 ± 0.36 (0.02)	0.10 ± 0.65 (0.03)	-2.15 ± 0.61 (0.03)
Gln493	His34	-0.95 ± 0.28 (0.01)	-1.43 ± 1.25 (0.06)	-2.10 ± 1.47 (0.07)
Phe486	Tyr83	-1.00 ± 0.37 (0.02)	-0.39 ± 0.21 (0.01)	-2.05 ± 0.65 (0.03)
Tyr495	Lys353	-0.04 ± 0.35 (0.02)	-3.88 ± 4.57 (0.20)	-2.04 ± 2.27 (0.10)

The interaction RBD Gln498 - hACE2 Asp38 is disrupted by lisinopril, and there is a notable increase in the average pairwise decomposition energy of this interaction. It is possible

that the formation of a van der Waals interaction and a hydrogen bond between lisinopril and hACE2 Glu37, the residue next to hACE2 Asp38, interferes with this interaction. Additionally, lisinopril decreases the percent occurrence of the hydrogen bonding interactions RBD Gln498 - hACE2 Asp38, RBD Gln498 - hACE2 Lys353, and RBD Gly496 - hACE2 Lys353. Similar to the other ligands, the decrease in the hydrogen bond occurrence of these interactions could be due to the formation of new hydrogen bonding interactions involving lisinopril. Table S22 contains the significant hydrogen bonding interactions between lisinopril and the complex; however, these interactions do not involve residues that are present in the previously mentioned disrupted interactions.

Additionally, the percent occurrence of the hydrogen bonds RBD Tyr505 - hACE2 Glu37, RBD Thr500 - hACE2 Asp355, RBD Tyr489 - hACE2 Tyr83, and RBD Tyr495 - hACE2 Lys353 were increased in the lisinopril-bound complex. Table S23 contains the average pairwise decomposition energies for interactions between the RBD and hACE2 with energies less than -2 kcal/mol when lisinopril is bound in the interface. There is a prominent decrease in average pairwise decomposition energies of the following interactions: RBD Tyr505 - hACE2 Glu37, RBD Thr500 - hACE2 Asp355, and RBD Tyr495 - hACE2. This information suggests that lisinopril stabilizes these interactions. Interestingly, a significant interaction between lisinopril and hACE2 Glu37 occurs with an average pairwise decomposition of -2.78 (0.16) kcal/mol. Table S22 details that a hydrogen bond forms between hACE2 Glu37 and the nitrogen of the lysine-like functional group (N2) on lisinopril for 28.58% of the simulation. Also, there is a decrease in the average pairwise decomposition energy of the interaction RBD Lys417 - hACE2 Asp30 when lisinopril is bound in the interface due to the decrease in the average electrostatic energy. Similarly, lisinopril forms significant electrostatic and van der Waals interactions with RBD Lys417 and hACE2 Asp30, respectively. The average pairwise decomposition energies of lisinopril's interaction with RBD Lys417 and hACE2 Asp30 are -5.29 (0.27) and -4.46 (0.21) kcal/mol, respectively. The formation of strong interactions between residues and lisinopril could cause a change in the distance between RBD and hACE2 residues or decrease the RBD and hACE2 interactions' competition.

Further Analysis

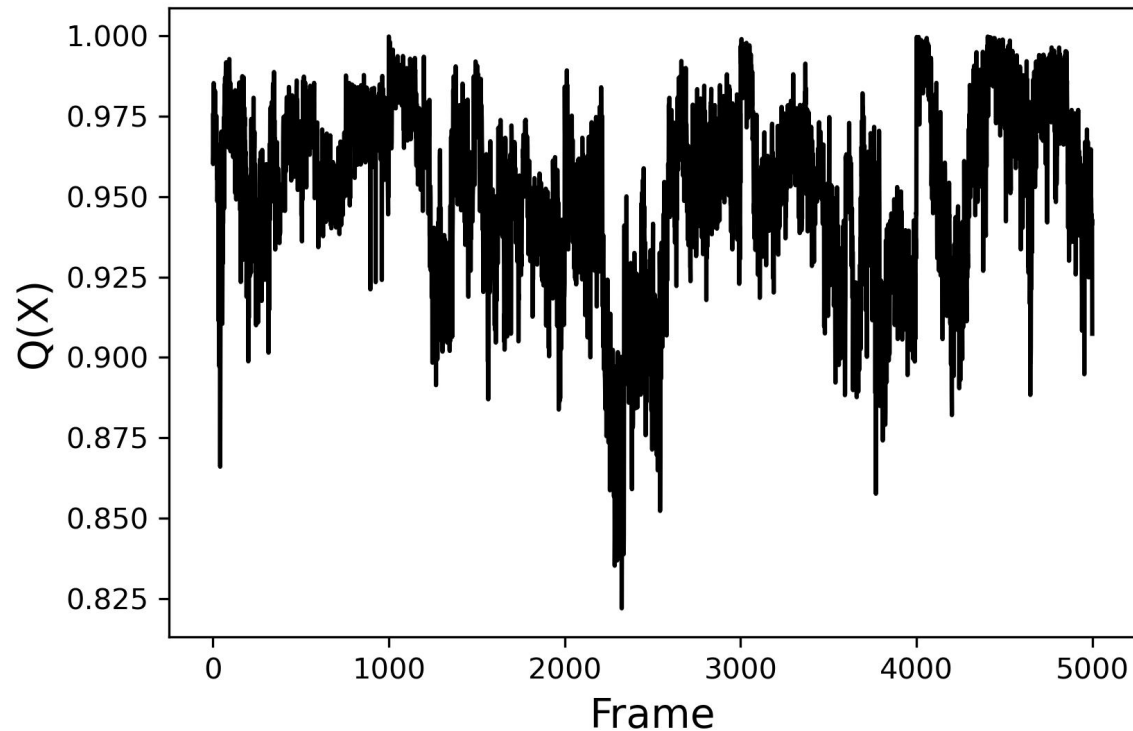


Figure S9. Native contact analysis in the interface of fosinopril bound complex 500 ns ensemble. The average fraction of native contacts for the 500 ns ensemble was 0.952 ± 0.027 .

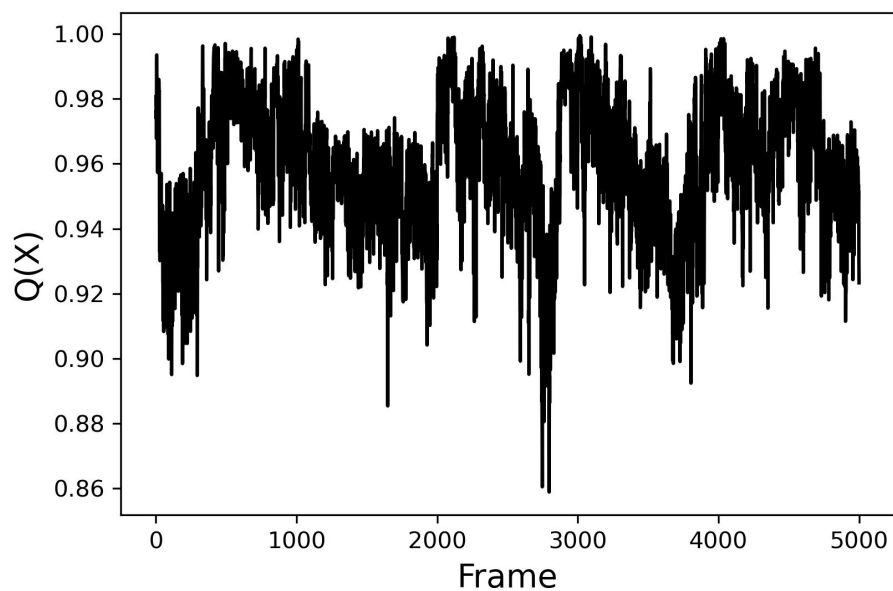


Figure S10. Native contact analysis in the interface of fosinoprilat in pose 2 bound complex 500 ns ensemble. The average fraction of native contacts for the 500 ns ensemble was 0.959 ± 0.021 .

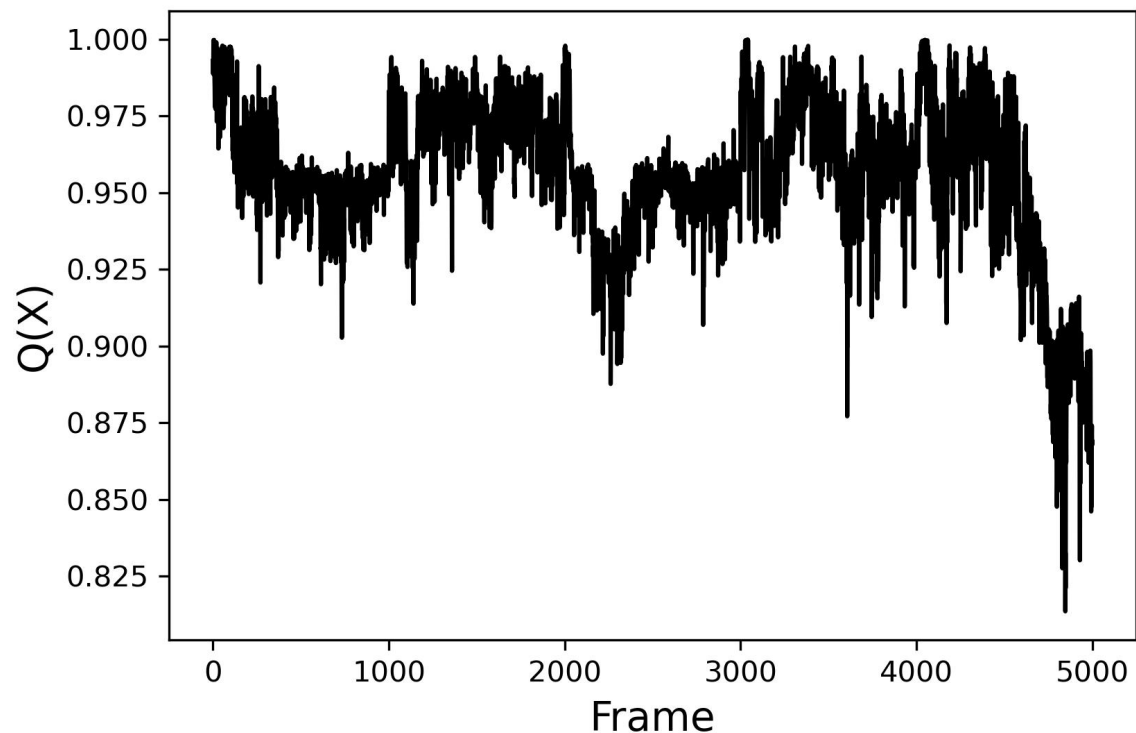


Figure S11. Native contact analysis in the interface of fosinoprilat in pose 3 bound complex 500 ns ensemble. The average fraction of native contacts for the 500 ns ensemble was 0.956 ± 0.024 .

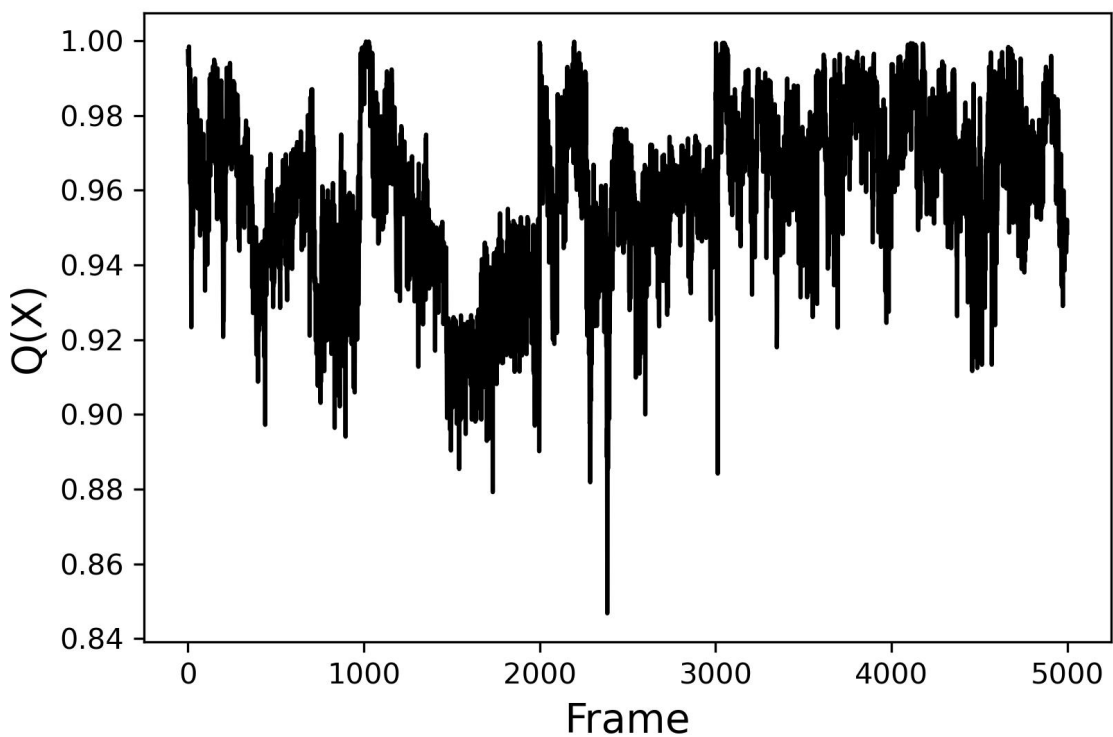
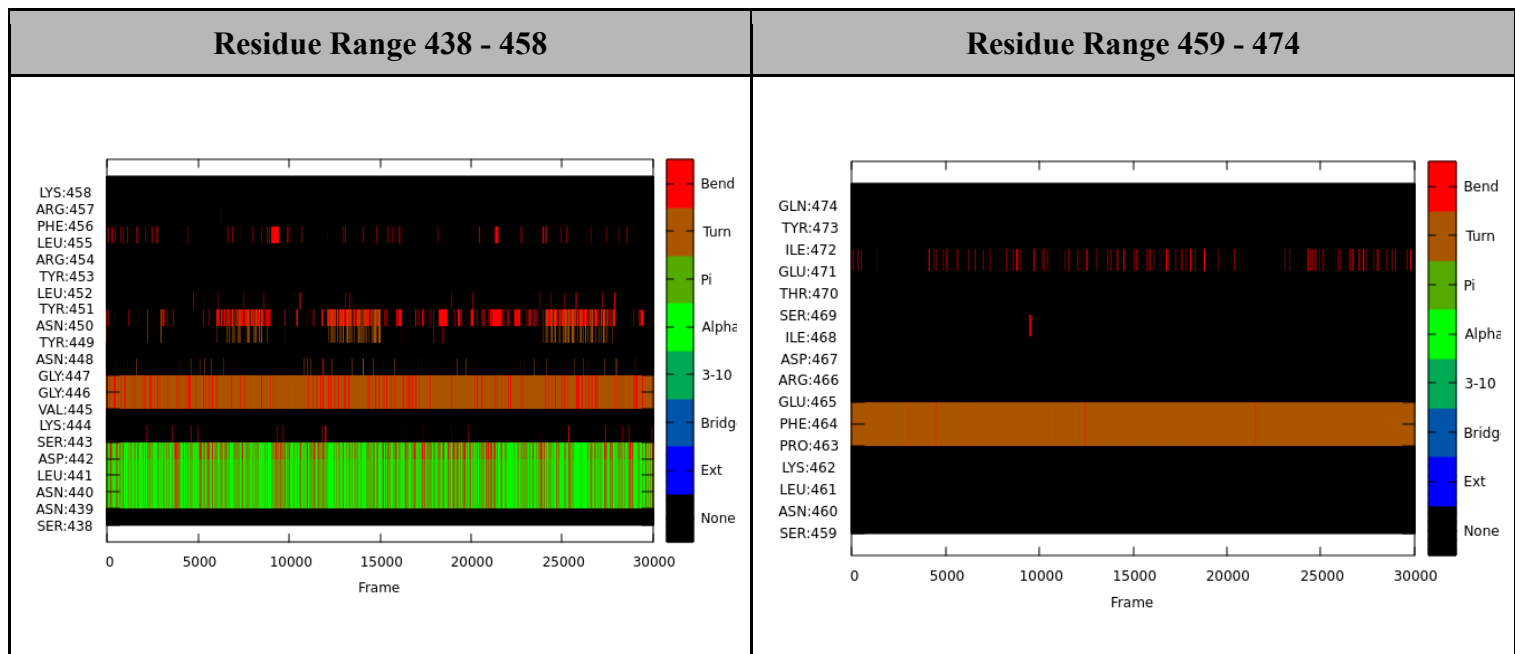


Figure S12. Native contact analysis in the interface of lisinopril bound complex 500 ns ensemble. The average fraction of native contacts for the 500 ns ensemble was 0.959 ± 0.022 .

Table S24. Secondary structure plots of RBM residues for the apo complex.



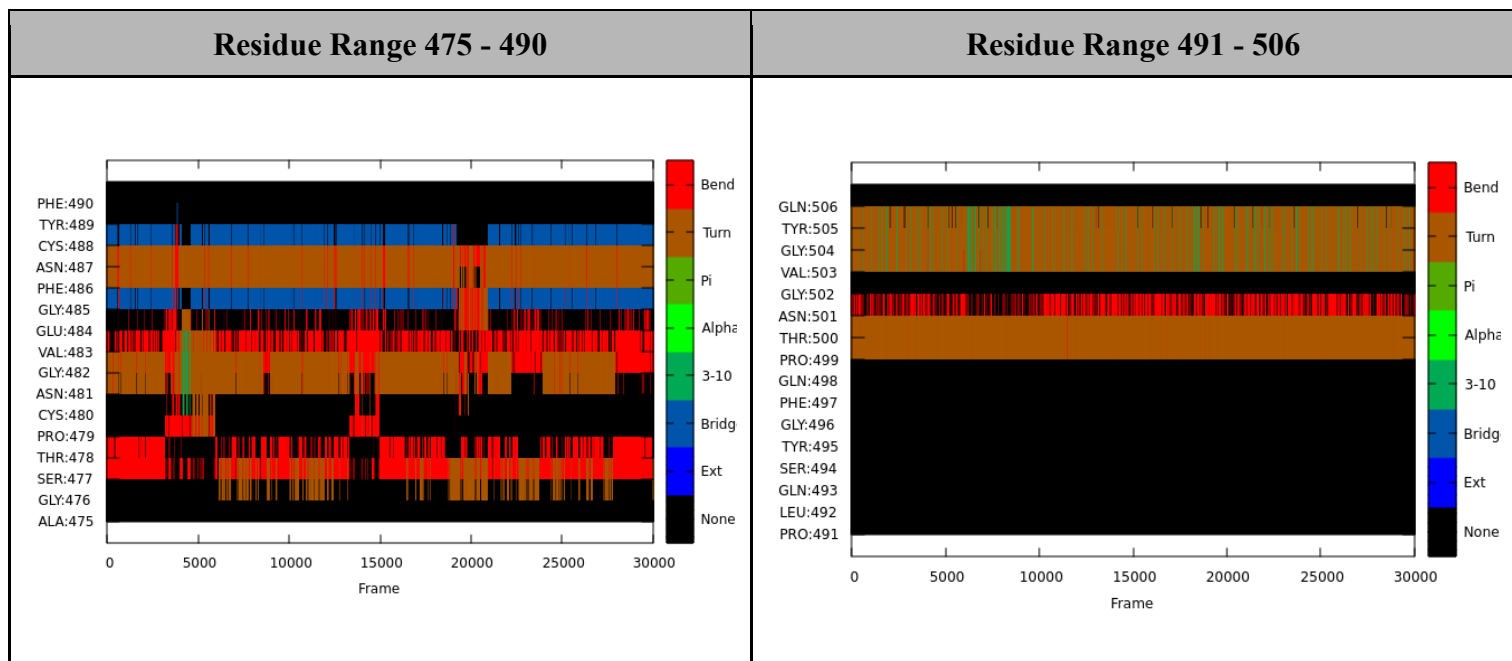
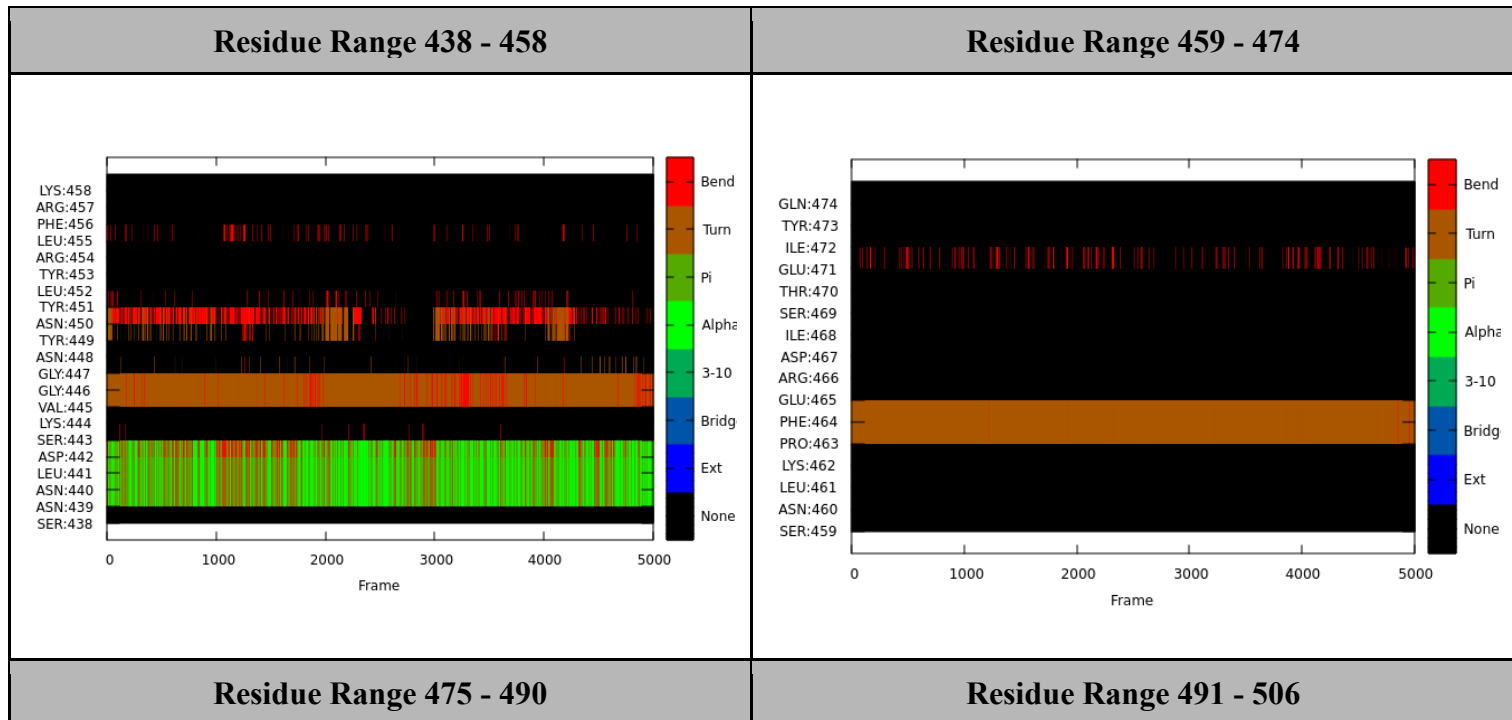


Table S25. Secondary structure plots of RBM residues for the fosinopril bound complex.



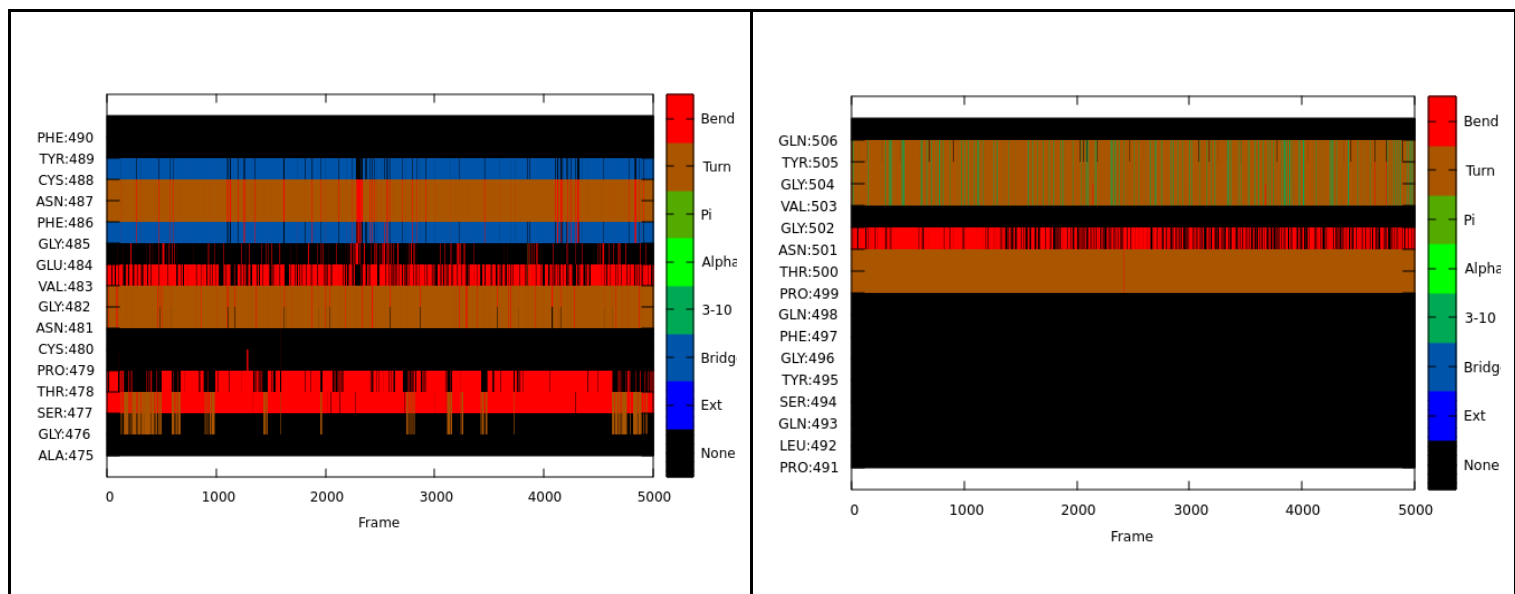
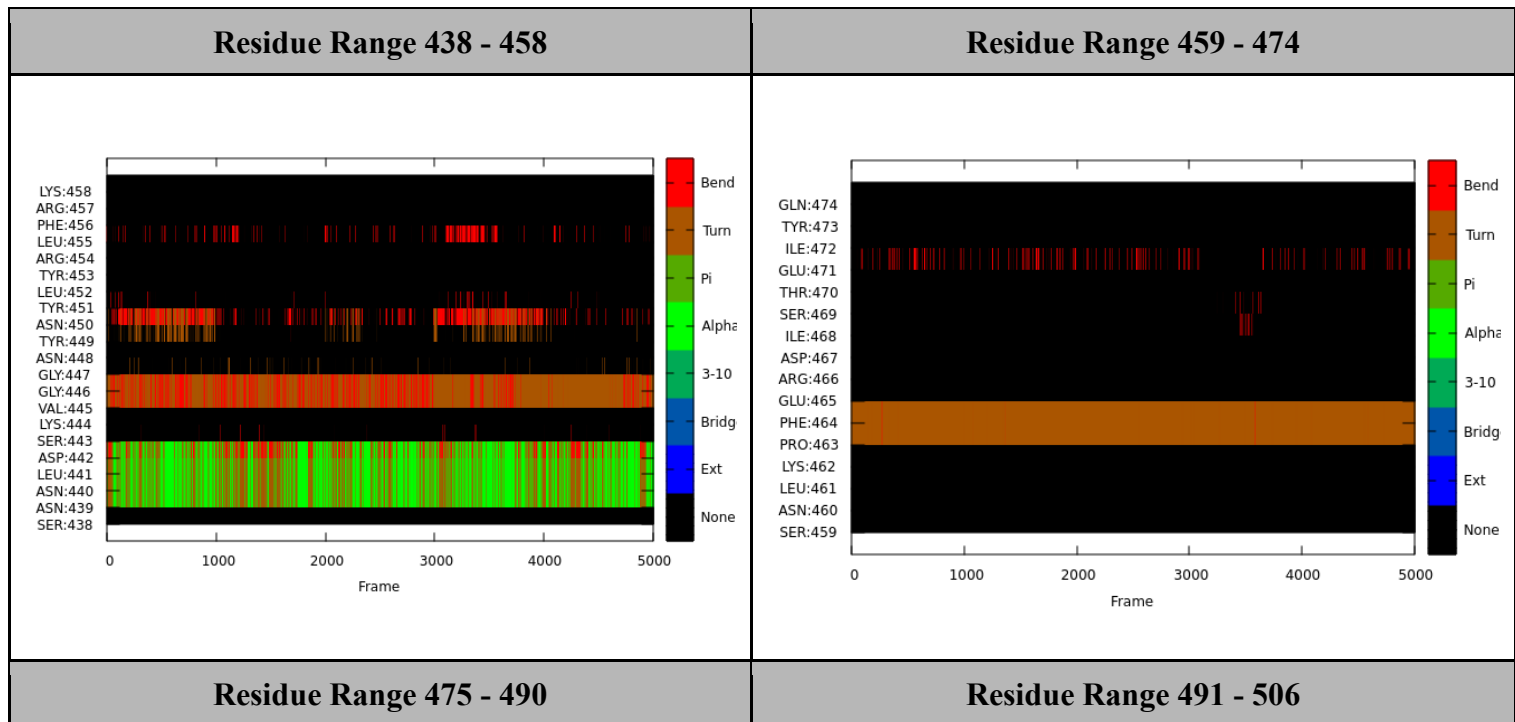


Table S26. Secondary structure plots of RBM residues for the fosinoprilat pose 2 bound complex.



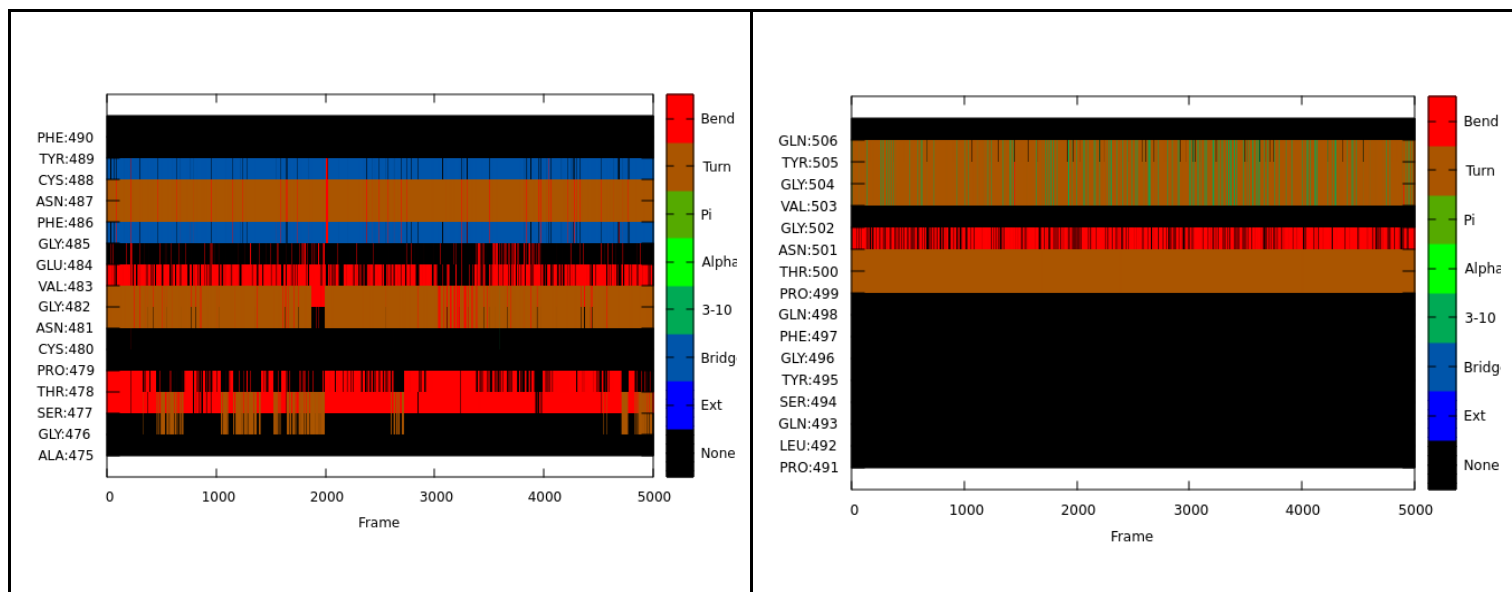
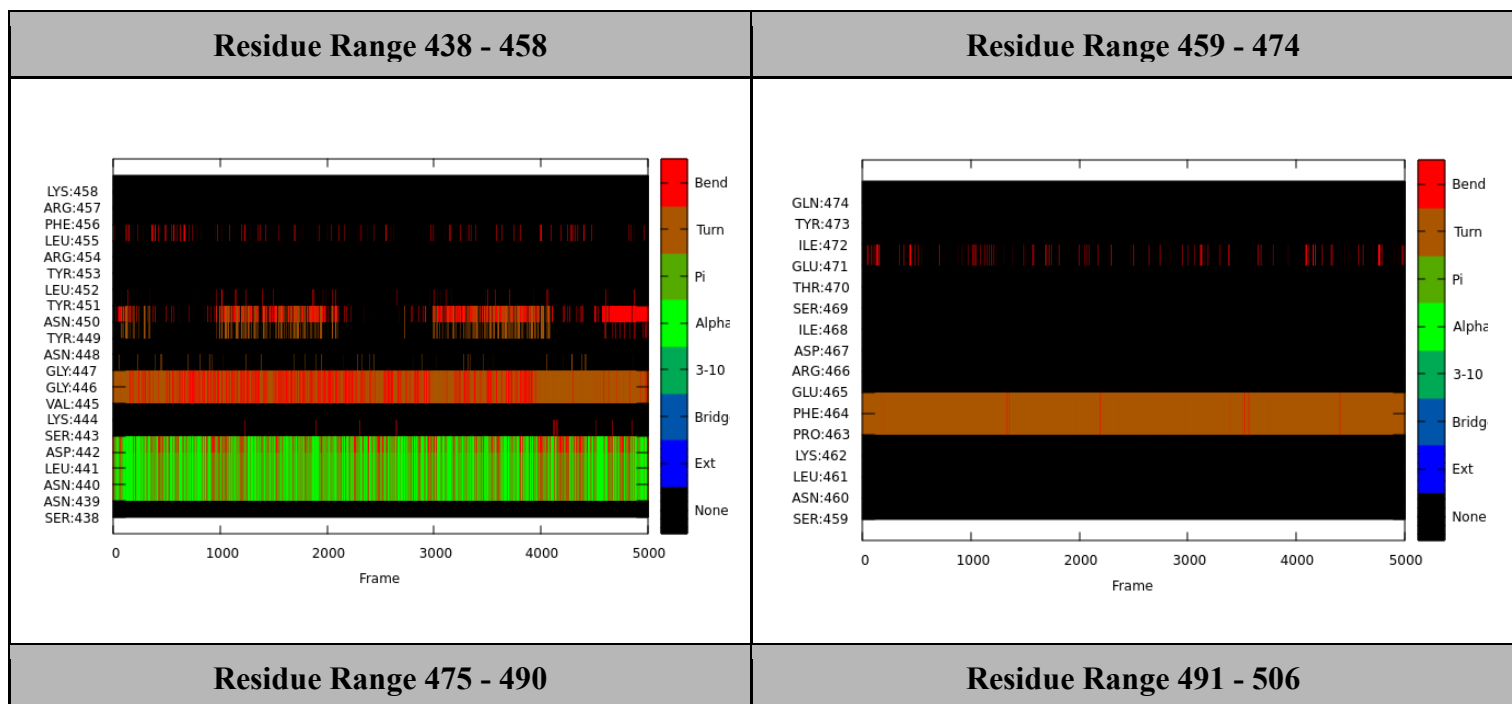


Table S27. Secondary structure plots of RBM residues for the fosinoprilat pose 3 complex.



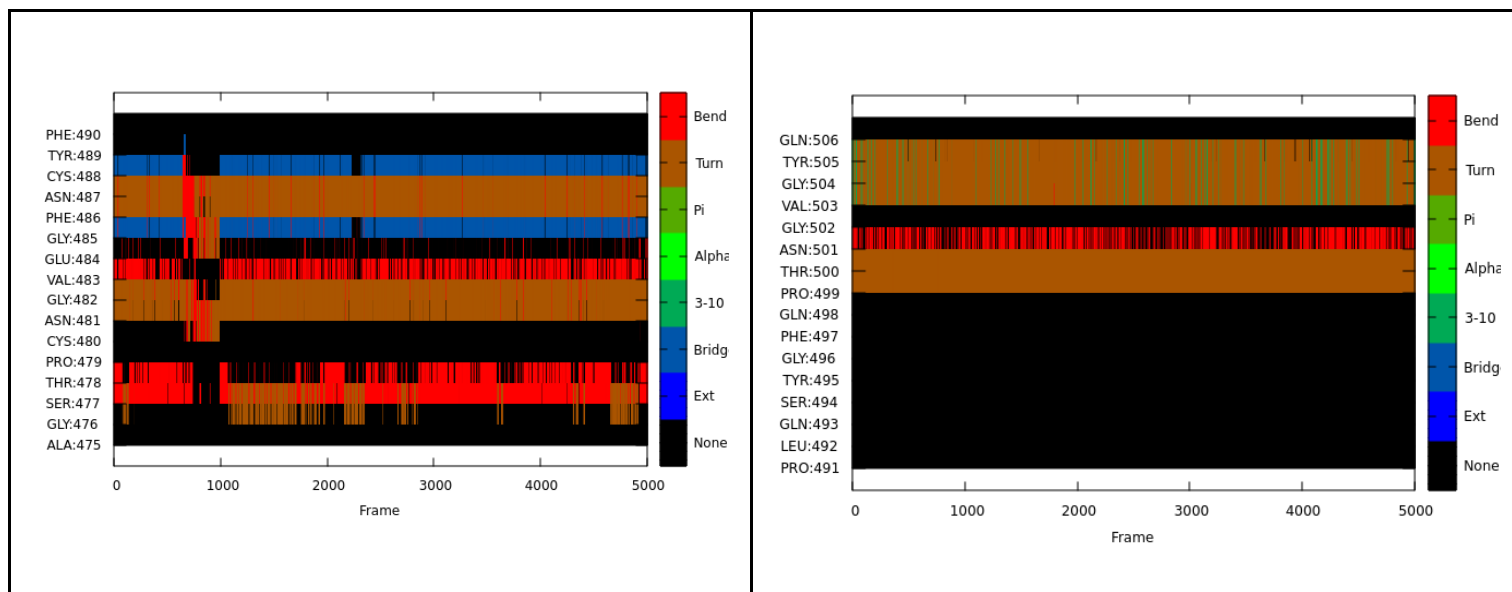
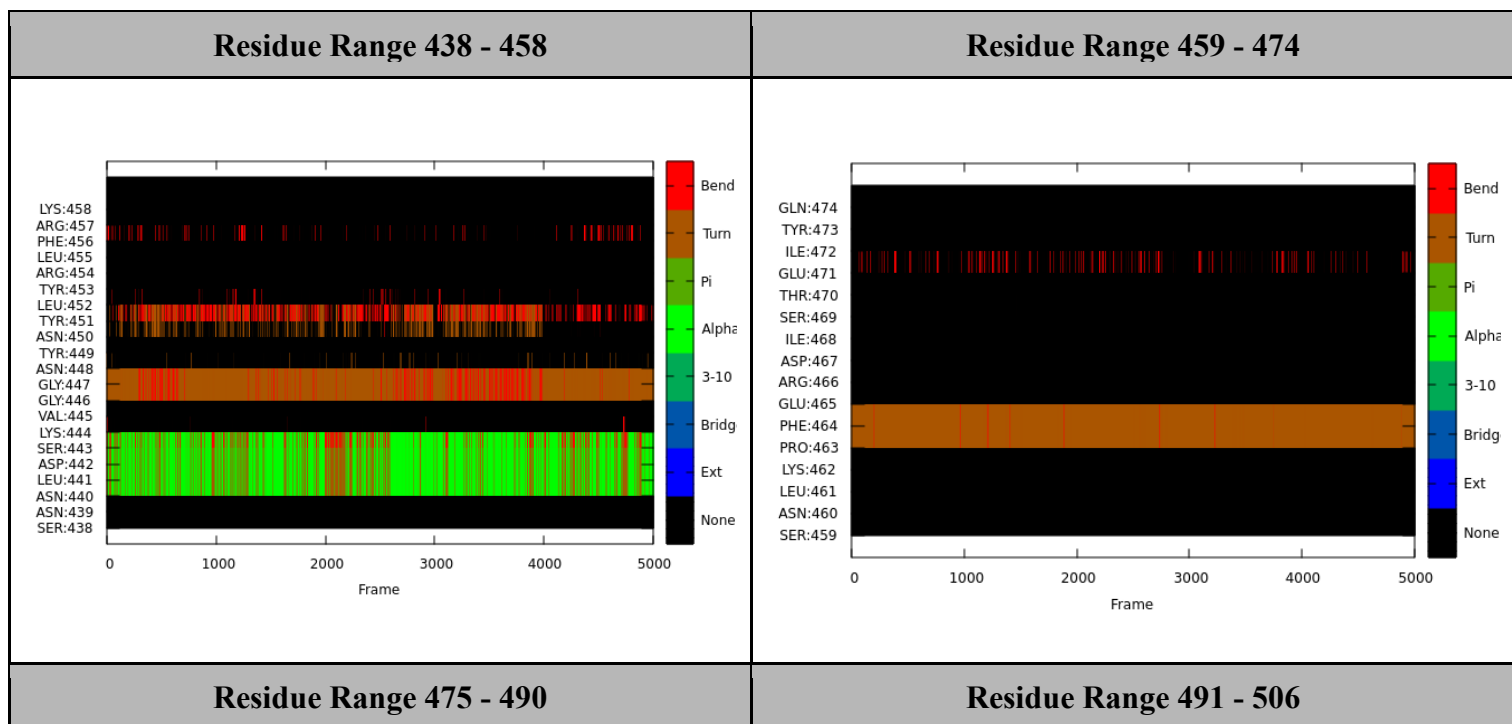


Table S28. Secondary structure plots of RBM residues for the lisinopril bound complex.



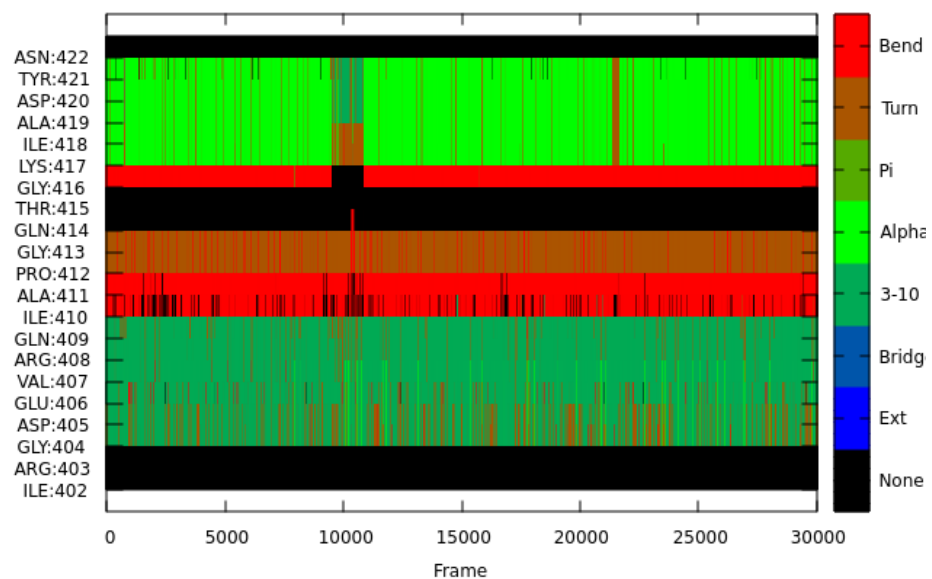
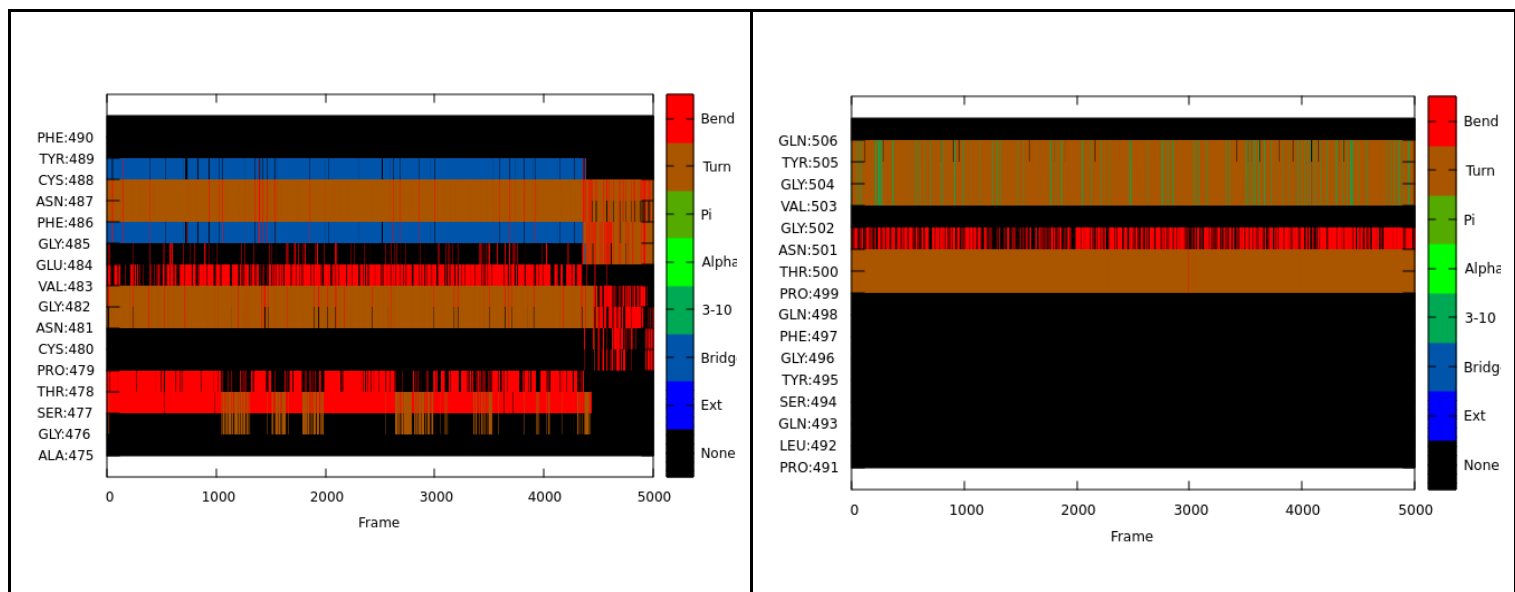


Figure S13. Secondary structure plot of residues 402 - 422 for the apo complex.

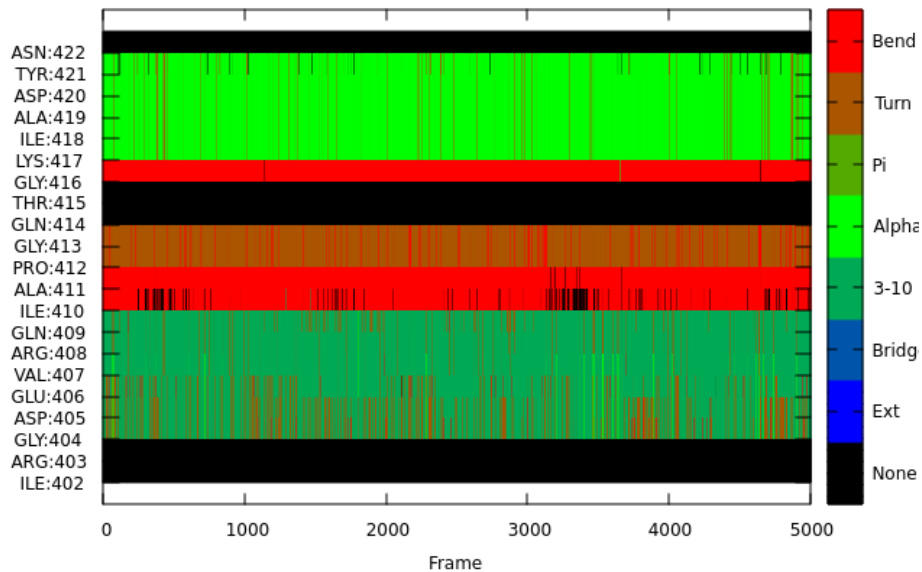


Figure S14. Secondary structure plot of residues 402 - 422 for the fosinopril bound complex.

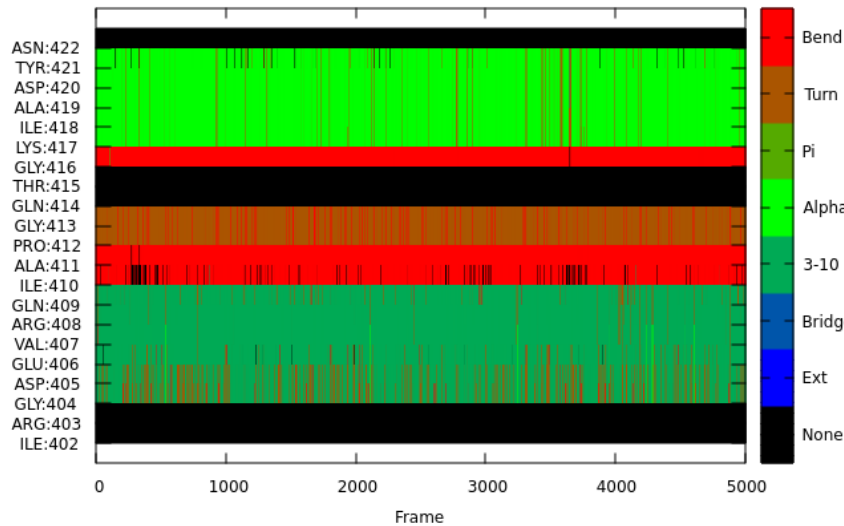


Figure S15. Secondary structure plot of residues 402 - 422 for the fosinoprilat pose 2 bound complex.

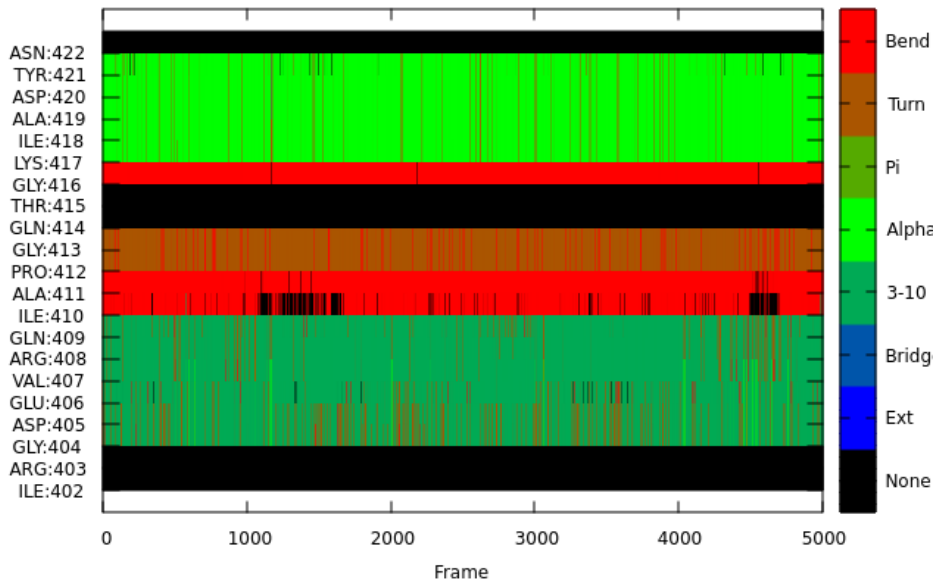


Figure S16. Secondary structure plot of residues 402 - 422 for the fosinoprilat pose 3 bound complex.

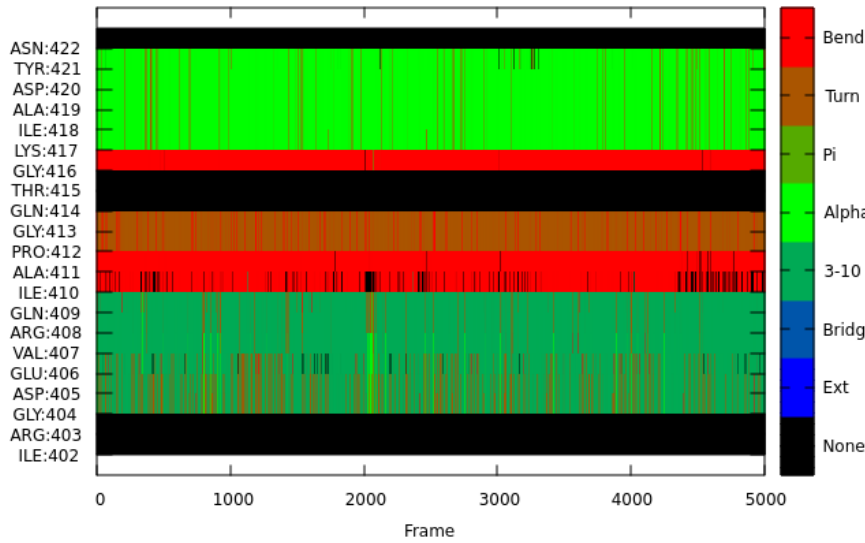


Figure S17. Secondary structure plot of residues 402 - 422 for the lisinopril bound complex.

Tables S24 - S28 contain the secondary structure plots for the apo and ligand-bound complexes for the residue range Ser438 - Gln506. For all ligand-bound complexes, there is a decrease in 3-10 helical occurrence for the residues Pro479 - Val483; however, notably, the helical structure of the apo complex was not present in a significant number of frames

throughout the 3 μs ensemble. There is a notable decrease in bend occurrence for the residue Gly482 for all ligand-bound complexes, with 23.93% as the apo ensemble occurrence and 3.82, 7.68, 4.86, and 8.24% as the fosinopril, fosinoprilat pose 2, fosinoprilat pose 3, and lisinopril ligand-bound ensemble occurrences, respectively. Additionally, there is an increase in turn occurrence for the residues Cys481 and Gly482 for the ligand-bound ensembles. The turn occurrences for the residues Cys481 in the apo ensemble is 74.22%, while the turn occurrence of this residue for fosinopril, fosinoprilat pose 2, fosinoprilat pose 3, and lisinopril ligand-bound ensemble are 96.18, 92.24, 94.80, and 86.86%, respectively. Similarly, turn occurrences for the residues Gly482 in the apo ensemble is 73.93%; while the turn occurrence of this residue for fosinopril, fosinoprilat pose 2, fosinoprilat pose 3, and lisinopril ligand-bound ensemble are 96.18, 92.24, 91.72, and 86.84%. Also, for the fosinopril ligand-bound ensemble, we noticed an increase in the bend occurrence for Asn450, where the occurrence increased from 28.99% in the apo ensemble to 43.34%. These differences in secondary structure occurrence could be caused by the ligand in the interface. The additional interactions between the ligand and the RBD could decrease the stability of the RBD structure by causing a decrease in helical and bend occurrence; however, it may have stabilizing effects by increasing the turn occurrence in all ligand-bound ensembles for the previously mentioned residues. To confirm the effect of the ligand on the RBD structure, it would be beneficial to extend the MD simulations in future studies.

Interestingly, the average position of each ligand is not near the previously mentioned amino acids where we notice a change in secondary structure, so we also decided to run a secondary structure analysis on the residue range Ile402 to Asn422. This range includes RBD amino acids that were found to have significant hydrogen bonding interactions with each ligand. Figures SD - SH are the secondary structure plots of the residue range Ile402 to Asn422 for the apo and ligand-bound complexes. From this analysis, we did not identify a significant change in secondary structure and believe that the extension of the ligand-bound MD simulations would be necessary to conclude the ligands' effect on the structure of the residues 402 to 422.

Table S29. Fosinopril water-mediated interactions. This table includes the percentage of water-mediated interactions between fosinopril and RBD residues or fosinopril and hACE2 residues. In a few cases, the water bridges an interaction between two residues and fosinopril; in this case, two residues are listed.

Residues involved in a water-mediated hydrogen bond	Hydrogen Bond Percent Occurrence
RBD Asp405	29.44
RBD Glu406	15.44
RBD Asp405 and RBD Gln409	9.98
RBD Arg403	9.88

hACE2 Ala387	8.98
RBD Gln409	7.66
RBD Arg408	7.52
hACE2 Glycan	5.62

Table S30. Fosinoprilat Pose 2 water-mediated interactions. This table includes the percentage of water-mediated interactions between fosinoprilat pose 2 and RBD residues or fosinoprilat pose 2 and hACE2 residues. In a few cases, the water bridges an interaction between two residues and fosinoprilat pose 2; in this case, two residues are listed.

Residues involved in the water-mediated hydrogen bond	Hydrogen Bond Percent Occurrence
RBD Glu406	72.24
hACE2 Ala387	44.80
hACE2 Asp30	36.14
RBD Arg403	11.92
hACE2 Arg393	11.12
RBD Lys417	10.50
RBD Arg408	9.44
hACE2 Glycan	9.06
hACE2 His34	7.40
RBD Glu406 and RBD Arg408	7.24
hACE2 Asp30 and hACE2 Asn33	6.54
RBD Tyr505	5.80
hACE2 Gln388 and hACE2 Arg393	5.40

Table S31. Fosinoprilat Pose 3 water-mediated interactions. This table includes the percentage of water-mediated interactions between fosinoprilat pose 3 and RBD residues or fosinoprilat pose 3 and hACE2 residues. In a few cases, the water bridges an interaction between two residues and fosinoprilat pose 3; in this case, two residues are listed.

Residues involved in the water-mediated	Hydrogen Bond Percent Occurrence
---	----------------------------------

hydrogen bond	
hACE2 Asp30	29.08
RBD Glu406	22.30
RBD Asp405	17.20
RBD Arg408	16.58
RBD Lys417	14.40
hACE2 Ala387	10.96
hACE2 Glycan	9.86
hACE2 His34	7.38
RBD Arg403	7.28
hACE2 Asp30 and hACE2 Asn33	5.98
hACE2 Asp30 and hACE2 His34	5.56

Table S32. Lisinopril water-mediated interactions. This table includes the percentage of water-mediated interactions between lisinopril and RBD residues or lisinopril and hACE2 residues. In a few cases, the water bridges an interaction between two residues and lisinopril; in this case, two residues are listed.

Residues involved in the water-mediated hydrogen bond	Hydrogen Bond Percent Occurrence
RBD Glu406	33.72
hACE2 Ala387	20.42
hACE2 Asp30	14.06
RBD Arg408	10.74
RBD Arg403	10.12
RBD Lys417	9.14
hACE2 Glycan	8.54
hACE2 His34	8.24

RBD Asp405	5.82
RBD Asp405 and RBD Gln409	5.50